UNIVERSITÀ DEGLI STUDI DI TRIESTE

XXVIII CICLO DEL DOTTORATO DI RICERCA IN BIOLOGIA AMBIENTALE

DISTRIBUTION OF NANOPLANKTON AND PICOPLANKTON AND THEIR TROPHIC INTERACTION IN THE ROSS SEA

Settore scientifico-disciplinare: **Ecologia**

DOTTORANDO
MASSIMO MAVELLI

COORDINATORE
PROF. SERENA FONDA UMANI

SUPERVISORE DI TESI
PROF. SERENA FONDA UMANI

ANNO ACCADEMICO 2014 / 2015

Riassunto

Il Progetto Deep Ross finanziato dal PNRA (Progetto Nazionale di Ricerca in Antartide) si prefigge di migliorare le conoscenze relative al funzionamento degli ecosistemi della porzione più profonda del Mare di Ross (Antartide).

Un'approfondita conoscenza del funzionamento del ciclo del C in ambiente oceanico è fondamentale per predire le conseguenze di un incremento atmosferico nei livelli di CO_2. Tradizionalmente la porzione afotica della colonna d'acqua, che costituisce il 65% dell'intera biosfera, è indicata come un ecosistema puramente eterotrofo dove prevalgono processi di mineralizzazione di sostanza organica prodotta negli strati superficiali. Ad oggi nell'Oceano Meridionale ed in particolare nel Mare di Ross scarse sono le informazioni sul metabolismo e sulla biodiversità di microorganismi profondi. Il Mare di Ross è un sito di studio ottimale poiché 1) è un sistema di origine di diverse masse d'acqua dense con diverse caratteristiche potenzialmente implicate in una diversa quantità e qualità di materiale organico esportato al fondo e 2) tali masse d'acqua, convogliando nelle Antarctic Bottom Waters (AABW), fungono da motore per la circolazione oceanica ventilando il 60% dell'intera massa oceanica globale.

Il mio lavoro di ricerca è incluso nelle attività previste e finanziate da questo progetto.

In particolare, la mia attenzione si è concentrata su 1) l'attività di predazione del nanoplancton eterotrofo sui procarioti di profondità del Mare di Ross e 2) sulla distribuzione delle abbondanze e delle biomasse del nanoplancton e del picoplancton lungo la colonna d'acqua in aree diverse del Mare di Ross.

L'attività di predazione del nanoplancton eterotrofo è, insieme alla lisi virale, il meccanismo di controllo delle abbondanze, biomasse e diversità delle comunità procariotiche. Nel mio caso sono stati allestiti 13 esperimenti di diluizione dai colleghi imbarcati durante la crociera sulla M/N Italica nel Mare di Ross nell'estate australe 2014. Per stimare il tasso di mortalità e di produzione procariotica si è utilizzato il metodo di Landry e Hasset (1982) adattato al comparto procariotico in 13 stazioni a quote a profondità variabile dai 1072m ai 200m. Per ciascuna stazione sono state allestite due serie di 4 diluizioni (100%, 80%, 50%, 10%). La serie T_0 è stata fissata immediatamente con formaldeide al 2% di concentrazione finale mentre la serie T_{24}

dopo 24 ore di incubazione. Per la valutazione della frazione pico- nanoplanctonica mi sono avvalso del protocollo Porter e Freig (1980) colorando i campioni con 4',6-Diamidino-2-fenilindolo (DAPI) e filtrandoli, successivamente, su filtri di policarbonato con porosità di 0,2 μm per picoplancton e 0,45 μm per nanolancton. Il conteggio è stato effettuato con un microscopio ad epifluorescenza utilizzando un filtro con lunghezza d'onda tra 330-385 nm per identificare gli organismi eterotrofi visibili grazie alla fissazione del colorante DAPI al DNA; gli organismi autotrofi sono stati visualizzati mediante l'utilizzo di un filtro con lunghezza d'onda compresa tra 520-550 nm in grado di sfruttare la naturale fluorescenza dei pigmenti fotosintetici.

Una volta ottenute le abbondanze cellulari (espresse in Cell L^{-1}), queste sono state trasformate in biomasse (μg C L^{-1}) mediante fattori di conversione.

Per ogni stazione sono stati stimati: il fattore di crescita, il fattore di predazione, la concentrazione iniziale della preda, la concentrazione media della preda durante l'esperimento, il tasso di ingestione, la produzione potenziale, la produzione reale, la produzione potenziale rimossa dalla predazione.

In 6 esperimenti (su 13) è stato possibile evidenziare una correlazione inversa tra crescita apparente e fattore di diluizione per cui è stato possibile calcolare il tasso di predazione che varia da 0.14 a 0.42 μg C $L^{-1}d^{-1}$. I tassi di predazione risultano relativamente alti rispetto ad esempio a quelli rilevati in profondità in Mediterraneo (Fonda Umani et al., 2010) dove però la temperatura è superiore ai 13°C, ciononostante soltanto in 3 dei 6 esperimenti superano la crescita apparente dei procarioti, indicando quindi un efficiente controllo top – down. Benchè gli esperimenti siano stati condotti utilizzando acqua di diversa origine (CDW, HSSW, AABW, ISW) i risultati positivi o negativi non sono associabili a nessuna ben definita massa d'acqua, né a specifiche profondità. Anche se i risultati sono significativi per meno della metà degli esperimenti, questi sono in assoluto i primi dati di flusso di C stimati in ambiente meso – batipelagico antartico e potranno essere di estrema utilità per eventuali usi modellistici.

Il secondo aspetto della mia ricerca ha riguardato la distribuzione delle abbondanze e delle biomasse del nanoplancton (autotrofo ed eterotrofo) e dei procarioti lungo la colonna d'acqua nelle 17 stazioni campionate. Il nanoplancton è stato anche suddiviso in classi dimensionali (2-3; 3-5; >5 μm).

Grazie ai dati forniti dalla sonda CTD (Conductivity Temperature Depth), utilizzata durante il campionamento, è stato possibile identificare le caratteristiche delle masse d'acqua ad ogni profondità di prelievo.

Per tutte le componenti considerate si osserva un drastico decremento delle abbondanze dalla superficie al fondo, come del resto atteso, anche se il decremento non è quasi mai del tutto lineare: per il nanoplancton si segnala un rilevante massimo sub-superficiale nella stazione 76 e una meno importante per il picoplancton nella stazione 30 – 31.

Ad ogni modo al di là di un generico decremento con la profondità, non si osserva nessun trend comune tra le abbondanze dei procarioti e quelle del nanoplancton, né andamenti specifici in specifiche masse d'acqua. Infatti, la cluster analisi applicata alla matrice contenente tutti i valori di abbondanza di pico- e nanoplancton in tutte le stazioni e a tutte le quote non genera un dendrogramma che separi chiaramente campioni appartenenti a specifiche masse d'acqua. Risultano soltanto strettamente associati fra loro numerosi (ma non tutti) campioni relativi alla CDW e circa la metà dei campioni prelevati nella AASW.

E' evidente che i soli valori quantitativi non sono sufficienti a identificare campioni appartenenti alla stessa massa d'acqua. Per ottenere una buona ripartizione è necessario disporre di dati qualitativi che non erano però obiettivo previsto dalla mia ricerca.

Summary

Recent study highlighted the important role of microorganisms in the marine ecosystem not only in the degradation of organic matter and release of biogenic elements but also as producers of organic matter. Microorganisms, in fact, control carbon fluxes in the ocean and in the coastal areas. The structural partitioning into different size classes of planktonic organisms is of fundamental importance in driving organic carbon fluxes along pelagic food webs. For all these reasons, in the lasts decades, the interest in the study of deep marine ecosystem has sharply increased. This study focuses on the interaction of the picoplankton with the nanoplankton within the southern oceans trophic web and their relation within the main different water masses.

17 samples stations were identified and collected during the Deepross Project within the XXIX expedition of the Italian National program of Antarctic Research in the Ross Sea. This location was chosen for many reasons, but the most important is because the Ross Sea is the place of origin of different dense water masses that can influence the worldwide oceans and the information on the biodiversity and the metabolism of deep microorganisms are very scarce.

Experiments of predation were performed at 13 stations using the dilution method following the Landry and Hasset protocol as updated by Landry in 1995. Two series of 4 dilutions (100%, 80%, 50%, 10%) were set for each stations, one was fixed immediately (T0) with formaldehyde at 2% final concentration and the other one after 24 hours of incubation (T24). To estimate the picoplanktonic and nanoplanktonic fractions we follow the Porter and Freig protocol (1980) staining the samples with 4',6-diamidino-2-phenylindole (DAPI), filtering the picoplankton on 0.2 μm mesh size and the nanoplankton on 0.45 μm mesh size, and counting them with an epifluorescence microscope.

At lest 100 - 200 organism were counted in each filter to estimate the abundances that was converted in carbon biomass using conversion factors.

Nanoplankton were counted and divided in three dimensional classes (2-3 μm, 3-5 μm and 5-10 μm). For each station we estimated: growth factor, grazing factor, initial

concentration of the prey, mean concentration of the prey during the experiment, ingestion rate, potential production, real production, potential production removed by grazing, initial standing stock removed by grazing.

The results of the grazing experiments showed as the picoplankton was significantly affected by the grazing pressure in only 6 out of 13 stations. Although grazing rates were relatively high if compared to those measured in the meso – bathypelagic Mediterranean regions (Fonda Umani et a., 2010), only in 3 stations grazing rate exceeded growth rate, indicating an intense top – down control. Nevertheless of the few significant data on C fluxes we have to keep in mind that these are the first data for the Ross Sea interior, which will be useful for the eventual modelling exercises.

I analysed the vertical distribution of abundance (and biomass) of pico- and nanoplankton along the water column at 17 stations in the Ross Sea.

The most relevant result is the drastic decrease of both fractions from the surface toward the bottom, although not always perfectly linear. I did not observe any common trend for pico- and nanoplankton at any of the stations.
Indeed cluster analysis applied to the pico – and nanoplankton abundance matrix of all samples, put in evidence only few correlations between specific water masses and abundance distribution (only part of the CDW and ASW samples appeared strictly associated). It is evident that abundance data alone are not useful to identify specific samples associations, which can be highlighted only by using qualitative data that were not part of my research.

INDEX

1. INTRODUCTION

1.1 THE SEVENTH CONTINENT

Of all continents the southernmost is the Antarctica, which contains the geographic South Pole and is considered the coldest, driest and windiest one. It is possible to define it as a frozen desert for its annual precipitation more or less of only 200 mm with very low temperature, which can reach -89°C. It is so hostile and remote that it has no native populations. Antarctica is surrounded by the Southern Ocean, and it covers more than 14.000.000 km^2, making it the fifth-largest continent, about 1.3 times as large as Europe. The coastline measures 17,968 km (11,165 mi) and is mostly characterized by ice formations. Antarctica has a number of mountain summits, including the Transantarctic Mountains, which divide the continent into eastern and western regions. A few of these summits reach altitudes of more than 4,500 meters (14,764 feet). The elevation of the Antarctic Ice Sheet itself is about 2,000 meters (6,562 feet) and reaches 4,000 meters (13,123 feet) above sea level near the center of the continent. Antarctica is divided into two main areas - East Antarctica and West Antarctica separated by the Transantarctic Mountains that stretch 3,540 kilometres across the continent.

About 99% of Antarctica is covered with a vast ice sheet. The ice sheet averages 2,450 metres deep and holds about 70% of the world's fresh water. With such a thick layer of ice, Antarctica is the highest of all the continents. The average altitude is about 2,300 metres above sea level, although in places, the bottom of the ice can be as much as 2,500m below sea level. If they were not filled with ice, large parts of Antarctica would be under the sea. Vinson Massif is Antarctica's highest point, rising to a height of 4,897 metres. Huge rivers of ice known as glaciers are

pulled slowly by gravity from the interior towards the sea. Along the way, the ice cracks, breaks and is ruptured by underlying rock.

On reaching the sea, the glaciers spill out over the water's surface and create gigantic floating blocks of ice called ice shelves. The largest, the Ross Ice Shelf, is the size of France. Sometimes pieces of an ice shelf break off to form icebergs. Beyond the ice shelves, much of the surrounding ocean freezes over during the winter. With this extra winter sea ice, Antarctica almost doubles in size.
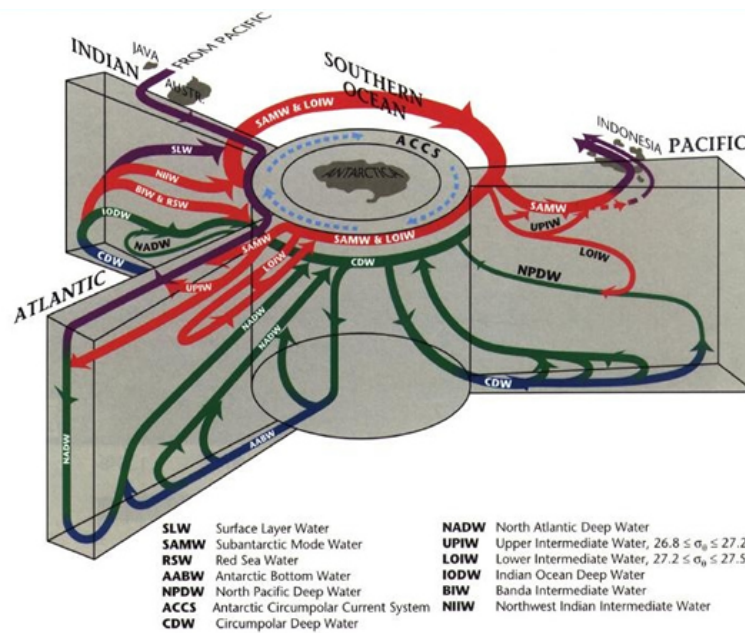
1.2   THE ROSS SEA

Placed between Cape Adare (170°E) and cape Colbeck (156°W), the continental shelf of the Ross Sea comprises a triangular area of about $5x10^5$ km^2 and mean depth of 500m, excluding the far southern portion covered by the Ross Sea Ice Shelf (RIS) which also extends to approximately $5x10^5$ km^2. The RIS is a 250 m thick ice cover that reaches half of the continental shelf and under which water flows freely in the ice cavity. Irregular topography is featured by shallow elevated banks and depressions reaching 1200m deep that behave as reservoirs of the salty and dense waters, since they are deeper than the continental shelf. The Ross Sea is the most biologically productive region of the Antarctic and is dominated by polinya processes (Fig. 1).

Fig. 1. The Ross Sea

1.2.1 Ross sea idrology and water masses

The continental margins of the Southern Ocean have long been recognized for their important water mass transformations and unique exchanges of heat and fresh water with the rest of the World Ocean (Wust, 1935; Deacon, 1937,1984) (Fig. 2).

Fig. 2. Principal southern ocean water masses and how they are linked with the world's oceans.

One of those regions is the Ross Sea. Among the various types of water masses that are generated in this place will be mention some of the most important.

The circulation of the Ross Sea is dominated by a wind-driven gyre, whose flow is strongly influenced by three submarine ridges that run in a southwest–northeast direction. Flow over the shelf below the surface layer consists of two anticyclonic gyres connected by a central cyclonic flow (Locarnini, 1994).

1.2.2 Antarctic Circumpolar Current (ACC)

An important dynamic feature of this sector of Southern Ocean is the Antarctic Circumpolar Current (ACC), which flows clockwise from west to east

around Antarctica creating the Ross gyre and interact with different water masses along its path (Deacon, 1984). The current is circumpolar due to the lack of any landmass connecting with Antarctica and this keeps warm ocean waters away from Antarctica, enabling the continent to maintain its huge ice sheet.

Associated with the Circumpolar Current is the Antarctic Convergence, where the cold Antarctic waters meet the warmer waters of the sub Antarctic creating a zone of upwelling nutrients. These nurture high levels of phytoplankton followed by copepods and krill, and resultant food chains supporting fish, whales, seals, penguins, albatrosses and other species.

The ACC connects the Atlantic, Pacific and Indian Ocean basins permitting a global overturning circulation to exist; the overturning circulation, in turn, dominates the global transport of heat, fresh water and other properties that influence the climate (Gordon *et al.,* 1990). Throughout its clockwise incursion, the ACC carries the most voluminouse water mass in the soutern ocean known as the Circumpolar Deep Water (CDW) (Budillon *et al.,* 2003; Orsi and Wiederwohl, 2009).

1.2.3 Circumpolar Deep Water (CDW)

Circumpolar Deep Water (CDW) is the most voluminous water masses in the southern Ocean (Worthington, 1981) a relatively warm, salty and nutrient-rich water mass that flows beyond the continental shelf at certain locations in the Ross Sea. This water is the result of a mixture of water formed in the Antarctic region and warm deep water flowing from the North Atlantic, Pacific and Indian oceans. CDW is identified by a temperature generally up to 1 °C with an average salinity of 34.65 (Jacobs *et al.,* 1970), for this reason moderates the ice cover through heat flux, provides a relatively warm subsurface environment for some organisms and provides nutrients to stimulate primary production. In the Southern Ocean the CDW takes part to the cyclonic circulation of the Ross Gyre (Locarnini, 1994; Orsi *et al.,*1995), interposing between the much colder Antarctic Surface Water (Mosby,1934) above and Antarctic Bottom Water below (Carmack,1977; Orsi *et al.,*1999).

1.2.4 Antarctic Bottom Water (AABW)

Antarctic Bottom Water (AABW) is the deepest water mass, which reaches the rest of the ocean from Antarctica. AABW is formed by the mixing of CDW with Antarctic Surface Water and water masses over the continental slope in the eastern Ross Sea, that goes down the slope to the ocean bottom (Foster and Carmack, 1976; Jacobs *et al.,* 1970). Is identified by a potential temperature and slinity range respectively of $-1.7 < \theta < 0$ and $34.65 < S < 34.72$ The production and northward export of AABW fill most of the World Ocean bottom layers, ventilating deep global ocean (Orsi *et al.,* 2002). The AABW formation is considered to happen at three regions around Antarctica: western Ross Sea, western Weddel Sea and Adelie Land close to the Mertez Glacier.

1.2.5 High Salinity Shelf Water (HSSW)

During wintertime, on the coastline, the cold katabatic wind could move the water surface ice, leaving surface water with high salinity and very low temperature. This kind of water mass is called High Salinity Shelf Water (HSSW) and is formed, generally, in proximity of polinyas and is characterized by salinities from 34.75 to 35 and temperature near the surface freezing point ($-1.91 < \theta < -1.85$°C) (Jacobs *et al.* 1985). HSSW accumulates in some places such as the Drygalski Basin, and part of this water is known to move along the Victoria and coast spreading in a slope near Cape Adare taking part to the formation of the Antarctic bottom water. Another part of the HSSW is well know to slide under the Ross Ice Shelf cavity leading to the formation of the Ice Shelf Water (ISW) (MacAyeal 1985, Jacobs *et al.* 1985).

1.2.6 Ice Shelf Water (ISW)

The southern part of HSSW flows under the RIS modifying themselves in Ice Shelf Water, this is due to the effects of cooling and melting at different depths, for this reason this water masses is characterized by a temperature lower than the freezing point ($\theta < -1.91$°C) at the surface pressure and salinity $34.62 < S < 34.70$. ISW come out from the RIS thereabout the Greenwich meridian and is primarily found on the central continental shelf of the Ross Sea (Budillon *et al.,* 2002; Jacobs *et al.,* 1985; Smethie and Jacobs, 2005), then it continues northward toward the shelf break to contribute to the formation of AABW (Jacobs *et al.,* 1985; Budillon *et al.,* 2011).
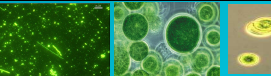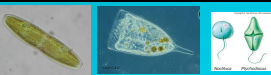
1.2.7 Antarctic surface Water (AASW)

Antarctic surface waters is characterized by temperatures higher than the freezing point and relatively lower salinity (34.2–34.4). AASW parameters are extremely variable, because it can be easily influenced by atmospheric conditions such as precipitation or ice dynamics. AASW is generally detected in the mixed layer (20 - 100m) of the oceanic regime, but it reach 400m near the cost along the upper continental slope east of the Ross Sea (Tonelli *et al.*, 2012).

1.3 PLANKTON

Plankton is the word used to refer to all those organisms living in the water column unable to swim against the current but moving passively in the water. This is a Greek word and it means, "vagabond", the German marine biologist Victor Hensen first coined it in 1887. Some of these are able to move, mainly vertically.

Plankton classification deeply changed in the last decades; in fact, despite large size organisms were well-known, the smallest part remained a mystery for a lot of time and only after the diffusion of the epifluorescence microscopy, that enabled a more detailed study on the smallest size of plankton organisms, was possible to put in evidence the importance of the massive presence of smallest plankton size as nanoplankton, picoplankton and femtonplankton.

According to this classification plankton is discerned in (Tab. 1):

Plankton	Size	Organisms	Organisms pictures
Femtoplankton	0,02 - 0,2 µm	Virus , Bacteria	
Picoplankton	0,2 - 2 µm	Bacteria, cyanobacteria, prochloropyta	
Nanoplankton	2 - 20 µm	Phytoflagellates, choanoflagellates, radiolarians, ciliates, metazoans	
Microplankton	20 - 200 µm	Diatoms, tintinnids, dinoflagellates, radiolarians, ciliates, metazoan	
Mesoplankton	2 - 20 mm	Crustaceans (copepods, euphausiacea, cladocerans)	
Macroplankton	2 - 20 cm	Jellyfish	
Megaplankton	20 - 200 cm	Jellyfish, colonies of tunicates	

Tab. 1. Plankton classification proposed by Sieburt *et al.,* 1978

6

Plankton can be distinguished in zooplankton (heterotrophic metabolism) and phytoplankton (autotrophic metabolism). Heterotrophic plankton requires carbon from organic sources and includes holoplankton (organisms that are planktonic for their entire life) and meroplankton (organism that spend only part of life as plankton). Autotrophs plankton synthesize nutrition from inorganic compound and consist of very small size organisms populating the euphotic zone of most oceans and freshwater ecosystems.

Phytoplankton is crucial not only for its role in the marine food web, but also because is one of major contributors of the global primary production. The importance of the two small (<20 μm) heterotrophic plankton groups in the structure and function of the ecosystem is associated with their involvement in the microbial loop, because they consume 20 - 60 % of primary production as dissolved and particulate organic matter (DOM and POM, respectively). Previous studies have shown that in hypoproductive regions, for example the Arctic, picoplankton and nanoplankton are responsible for up to 73% of Chl*a* concentrations, and their rapid turnover enables them to contribute substantially (83%) to total primary production (Agawin *et al.* 2002). The variation of some parameter like temperature (Zdanowski 1995; Price and Sowers, 2004; Doolittle *et al.,* 2008) and the sea ice dynamics (Becquevort et al., 2009; Lannuzel et al., 2013) can cause changes in the metabolism and rate of growth of planktonic organisms.

1.3.1 The trophic web and microbial loop

Primary production, biogeochemical process within the photic zone, and the pelagic food webs performances, play a primary role on the efficiency of carbon fluxes in the ocean and in the coastal areas

The structural partitioning into different size classes of planktonic organisms is of fundamental importance in driving organic carbon fluxes along pelagic food webs.

Until the end of the 70s scientists were in accordance to recognise that the relationship between the microphytoplanktonic primary production and their predators (mesozooplankton) regulate the flux of energy trough the trophic web.

In this prospective microphytoplanktonic organisms were the only responsible of the primary production and was not so clear that the loss of organic matter could have been the substrate for bacteria degradation (Azam, 1998).

This is the so-called "Classic pelagic food web" (Fig. 3) where microphytoplancton synthesize organic matter using the energy of the sun and transfer it to microzooplankton, these consumers are eaten by larger organisms (mesozooplankton). In this food web model, the carbon/energy move "linearly" to the higher trophic level (fish, birds).
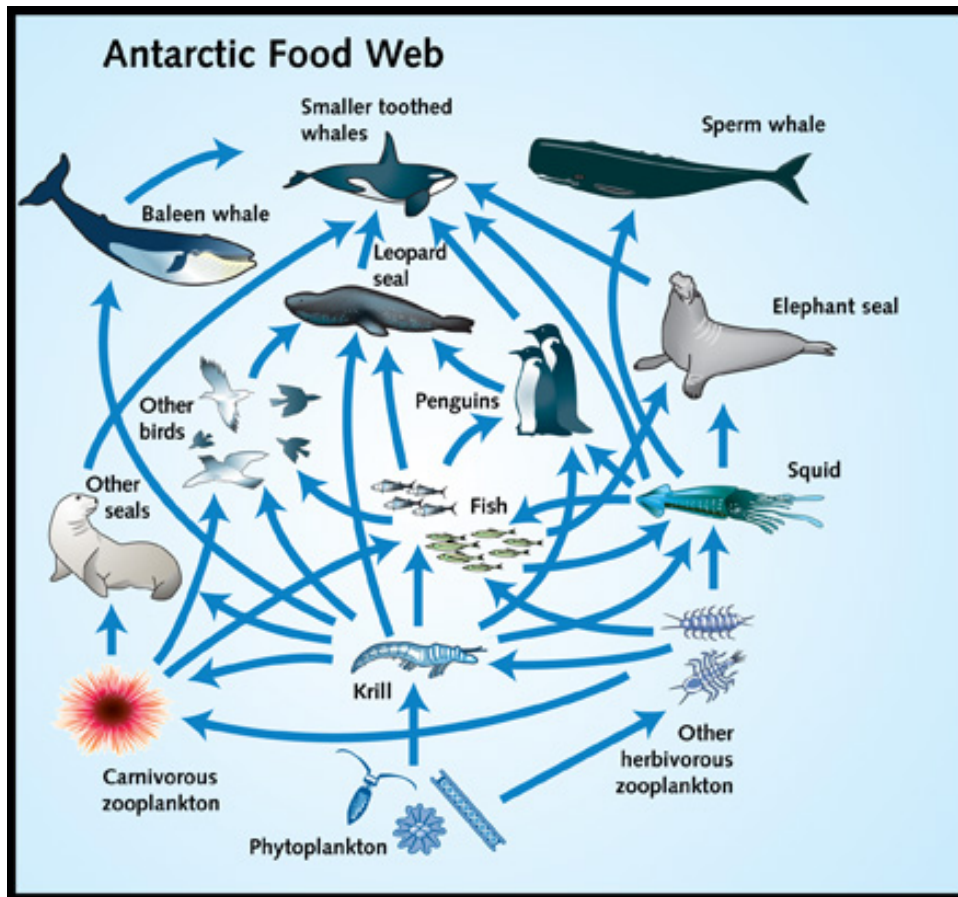

Fig. 3. Classic pelagic food web

Thanks to technology and research, more and new pieces are added to the intricate mosaic of the trophic web, the study on the oceans biogeochemical processes are increased and the idea of marine food web began to be revolutionized. Daley and

Hobbies in 1975, propose a new epifluorescence microscope technique that enhanced the study of marine bacteria highlighting the existence of enormous numbers of organisms in the range from 0.02 to 2μm including viral like particles and auto-heterotrophic bacteria (Pomeroy, 1974; Azam *et. al*., 1983; Rassoulzadegan, 1993; Legendre and Rassoulzadegan, 1995; Fonda Umani, 2000). The epifluorescence microscope gives the opportunity to discriminate autotrophic from heterotrophic microorganism, the first exploiting their natural fluorescence due to their photosynthetic pigments (Waterbury *et. al.,* 1979), the seconds by means of the new staining technique.

Bacteria are so abundant that is of primary importance in the pelagic trophic web (Pomeroy, 1974), prokaryotes are in fact the only organisms able to metabolize not only DOM (dissolved organic matter) and transform it into new biomass available for grazers (Azam *et. al.,* 1983) but also POM (particulate organic matter).The concept of "microbial loop" was introduced for the first time by Azam *et. al.,* in 1983 and was referred to the trophic interaction between pico-, nano- and microplankton where dissolved organic carbon (DOC) flows again to the higher trophic level thought its incorporation in bacterial biomass. DOC can be originated from different biological sources:

1) Cellular debris during grazing processes (sloppy feeding) (Eppley *et. al.,* 1981);

2) Cellular apoptosis;

3) Cellular lysis due to viral infection (Fuhrman and Noble, 1995);

4) Microalgal exudations (Williams, 1990; Alledredge *et al.,* 1993);

5) Faecal pellets degradation (Honio and Roman, 1978);

6) Enzymatic dissolution of marine aggregates

Bacteria act directly on the dissolved organic carbon (DOC) producing biomass that is grazed by heterotrophic nanoplankton and successively by microzooplankton. This chain of organisms replace the environment inorganic carbon (CO_2) by respiration and release DOC as well, closing in this way the loop. Nanoplankton can feed on both heterotrophic and autotrophic bacteria but also on small eukaryotic cells, whereas microzooplankton can utilize as a source of energy both the heterotrophic and autotrophic nano- and picoplankton fractions. In most cases the three food webs (classical, microbial and grazing) coexist within the so called mistivourous food web (Fonda Umani, 2000) (Fig. 4).
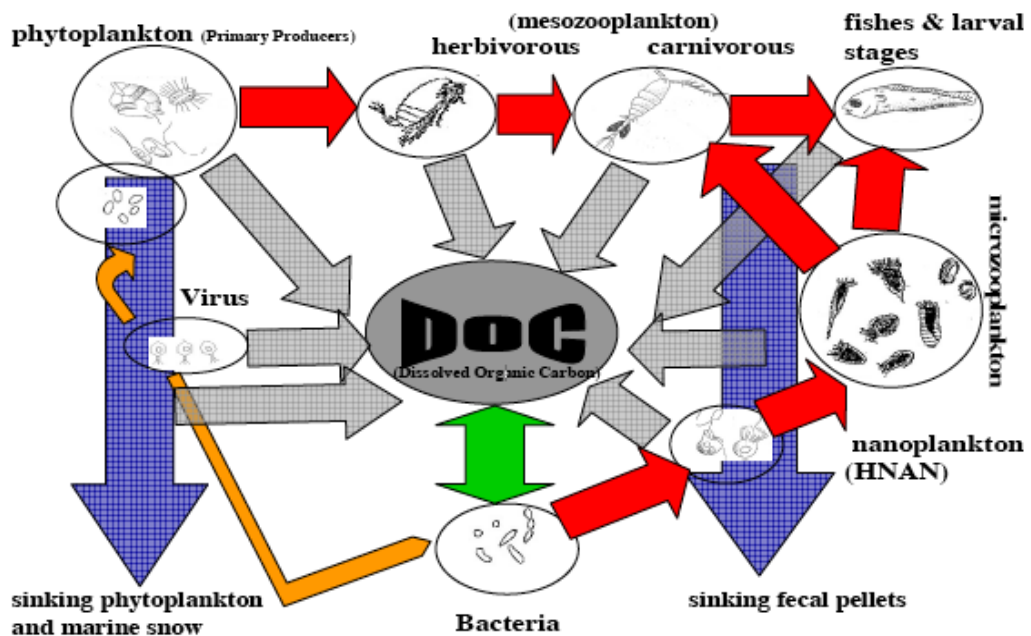
Fig. 4. Mistivourus food web

In the microbial loop, energy obtained from the substrate is immediately breathed or turned into faecal pellets with release of CO_2. With a predominance of classic food web the primary consumers retain organic carbon in their biomass producing faecal pellets that can settle on the seabed. Bacteria are of extremely importance in marine ecology especially because they are involved in the cycle of carbon and, consequently, in the exchange of CO_2 between the ocean and the atmosphere that can influence the global warming. Volk and Hoffert in 1985 identified 3 different kinds of "CO_2 Pumps":

1) Solubility Pump which is linked to the solubility of the carbon dioxide in the transitional layer between ocean and atmosphere and whose activity is joined to the deep-water formation.

2) Biological Pump which is strictly related to the marine food web and can interest the sedimentation of calcareus shell.

3) Soft tissue pump.

Biogenic carbon in the ocean were classified in relation to its turnover time defined as the time elapsed between the photosynthetic uptake of carbon and its return as CO_2 to the atmosphere (Legendre and LeFevre, 1992) and three main compartments have been defined: **short-lived organic** carbon that consists of organisms with short turnover times as well as labile dissolved organic compound, and it mainly transits through the "microbial food web"; it is properly represented by small phytoplankton, heterotrophic bacteria and protozoans. **Long-lived organic carbon** comprises renewable marine resources and transits through the "Classic food web" (Azam, 1998); it is represented by fish, marine mammals and also heterotrophic bacteria involved in the breakdown of organic matter derived from large heterotrophs. **Sequestered biogenic carbon** is present in different ways as organic remains buried in sediments, inorganic deposits of biogenic origin (e.g. calcareous ooze, coral reefs, continental limestone), refractory dissolved organic matter and dissolved CO_2 in deep waters resulting from the *in situ* oxidation (respiration) of organic compounds (Legendre, 1996).

Planktonic communities can shift from the prevalence of the microbial loop to the dominance of the classic food web over short-medium periods of time. Classic food web may occur in shallow turbulent environments, with strong hydro dynamism where nutrient availability is pulsed or episodic such as coastal areas or upwelling zones and where large boom of diatoms occur (Kiorbe, 1996).

Large size phytoplankton, whether actively fed by zooplankton with consequent excretion of relatively heavy faecal pellets, or sank by means of aggregation processes when inadequate feeding activity is present, cause a rapid removal of the fixed carbon from the photic layer. On the contrary, microbial food web is typical of low energy

environments, where the input of nutrients are scarce and the system is mostly based on regeneration processes (Kiorbe, 1996). As a consequence, the final fate of photosynthesised carbon can strongly change over time within the environment as function of planktonic food web structures.

1.3.2 Picoplankton

Picoplankton include microorganisms of size 0.2-2 microns (Christaki *et al.,* 2001) and can be distinguished in autotrophic and heterotrophic. In the pelagic ecosystem most of the marine biomass consists in eubacteria and archaea (bacteria). Bacteria are extremely important for the marine ecosystem, in fact they are involved in the carbon cycle of the world's oceans and are crucial in biogeochemical cycles of nutrients (N, P, Fe, S, Si) (Pomeroy *et al.*, 2007). Azam *et al*. (1984) demonstrated as bacteria activity on DOC, controls the fate of the fixed carbon in the ecosystem. Marine bacteria are present everywhere in the ocean and their abundance decreases by 2 orders of magnitudes from the surface to the sea bottom (Nagata *et al.,* 2000). Autotrophic bacteria are able to obtain nutrition from inorganic compounds and are most represented by prokaryotic phyla such Cyanobacteria (Johnson and Sieburth, 1979) with *Synechococcu*s and *Prochlorococcus* genera (Waterbury *et al.,* 1979; Chishlom *et al.*, 1988). *Synechoccus* could have cocci or rods shape, this could be a case of pleiomorphism related to the difference in light regime (Ahlgrem and Rocap, 2006; Palenik *et al*., 2006) and/or grazing pressure (Christaki *et al*., 1999, 2005), and its cell are dominant in the upper layer, on the contrary *Prochlorococcus* cells are most often found in deeper layer (Yacobi *et al.,* 1995). Antarctic picophytoplankton is composed primarily of eukaryotic flagellates (Agawin *et al.,* 2002). Heterotrophic bacteria instead use DOC, derived from phytoplankton, as source of energy. In the southern ocean marine heterotrophic picoplankton is dominated by bacterioplankton (Wynn-Williams, 1996; Simon *et al.,* 1999), whereas organisms from the domain Archea are not usually of substantial importance in surface waters during summer (2 %) and are more common in winter (13 - 34 %) (DeLong *et al.,* 1994; Murray *et al.,* 1998; Simon *et al.,* 1999; Church *et al.,* 2003).

1.3.3   Nanoplankton

Nanoplankton comprise the marine plankton fraction in the range of 2 - 10 μm. This size range includes autotrophic and heterotrophic microorganisms. They are considered almost omnivorous, in fact they could feed on picoplankton and other nanoplankton, and are considered the most relevant predators of picoplankton and make a top-down pressure on the smallest size fraction (Fenchel, 1982; Davis and Sieburth, 1984; Fuhram and McManus, 1984; Andersen and Fenchel, 1985; Kuuppo-Leinikki, 1990; Sherr *et al.,* 1989; Caron *et al.,* 1999; Fonda Umani *et al.,* 2005, 2010). Autotrophic nanoplankton are involved in primary production, while heterotrophic part feed on picoplankton fraction. Antarctic nanophytoplankton is dominated by eukaryotic flagellates, for example haptophytes (<60%), cryptophytes (<40 %), and prasinophytes (<17%), which are followed by small diatoms (<18 %) (Wright *et al.,* 2009) and dinoflagellates (<11 %). The nanoheterotrophs are composed of flagellate groups (30 % of the nanoplankton biomass), ciliates, and dinoflagellates (Hewes *et al.,* 1990; Azam *et al.,* 1991) An essential aspect of nanoplankton, which is preyed by microzooplankton, is its contribution to the flow the energy into the trophic web (Gasol, 1994; Sanders, 1991). They can have many different feeding strategies as sedimentation, filter feeding, interception feeding, raptorial feeding supported by pharynx or by pseudopod. Some of these strategies, as the ability to use pseudopod, could be an important factor to survive in place with low food concentration (Boenigk and Arndt, 2002). In environments with very low food concentrations they can adopt different strategies to survive as rapid encystment/excystment, modification in food sources or metabolic, cytological and physiological changes (Sleigh 2000).

1.4   AIM OF THE RESEARCH

Until now, the microbial dynamics and their interaction in the southern oceans trophic web is still an intriguing ecological enigma. This lack of information incites more and more researchers to fill this scientific gap collecting data from place like the Ross Sea, which is a hot spot of formation of different water masses that influence the climate and life of worldwide oceans. For this reason the goal of this work is to give a small contribution to better understanding the distribution of nano- and picoplankton within the different main Ross Water masses and quantify the carbon flux between pico- and nanoplankton in deep area of the Ross Sea during the austral summer.

2 MATERIALS AND METHODS

2.1 THE DEEPROSS PROJECT

The study presented in my PhD thesis was possible thanks to the samples collected during the Deepross Project within the XXIX expedition of the Italian National program of Antarctic research in the Ross Sea, on board of the M/N Italica, during the austral summer between 5th January and 5th February 2014.

The DEEPROSS PROJECT purpose is to increase and clarified the scientific knowledge on the dynamic of organic and inorganic carbon production and consumption in deep sea environment characterized by ocean ventilation. The comparison between data obtained in areas with different oceanographic characteristics could give new information on the impact of the quality and quantity of organic substance on the deep sea functionality. All this, represent the first attempt to better understand ecological, biological and physical dynamic of the surrounding deep sea environments.

2.1.1 The study area

Samples were collected in the Southern Ocean and precisely in the Ross Sea (Fig. 5). This area was chosen as the study area for many reasons:

1) It represent a place of origin of different dense water masses with different characteristics probably involved in the dislocation of organic matter, of different quantity and quality, to the sea bottom

2) Those water masses converging in to the Antarctic Bottom Water (AABW) that fill most of the World Ocean bottom layers, ventilating the 60 % of deep global ocean.

3) Very few information on the biodiversity and the metabolism of deep microorganisms
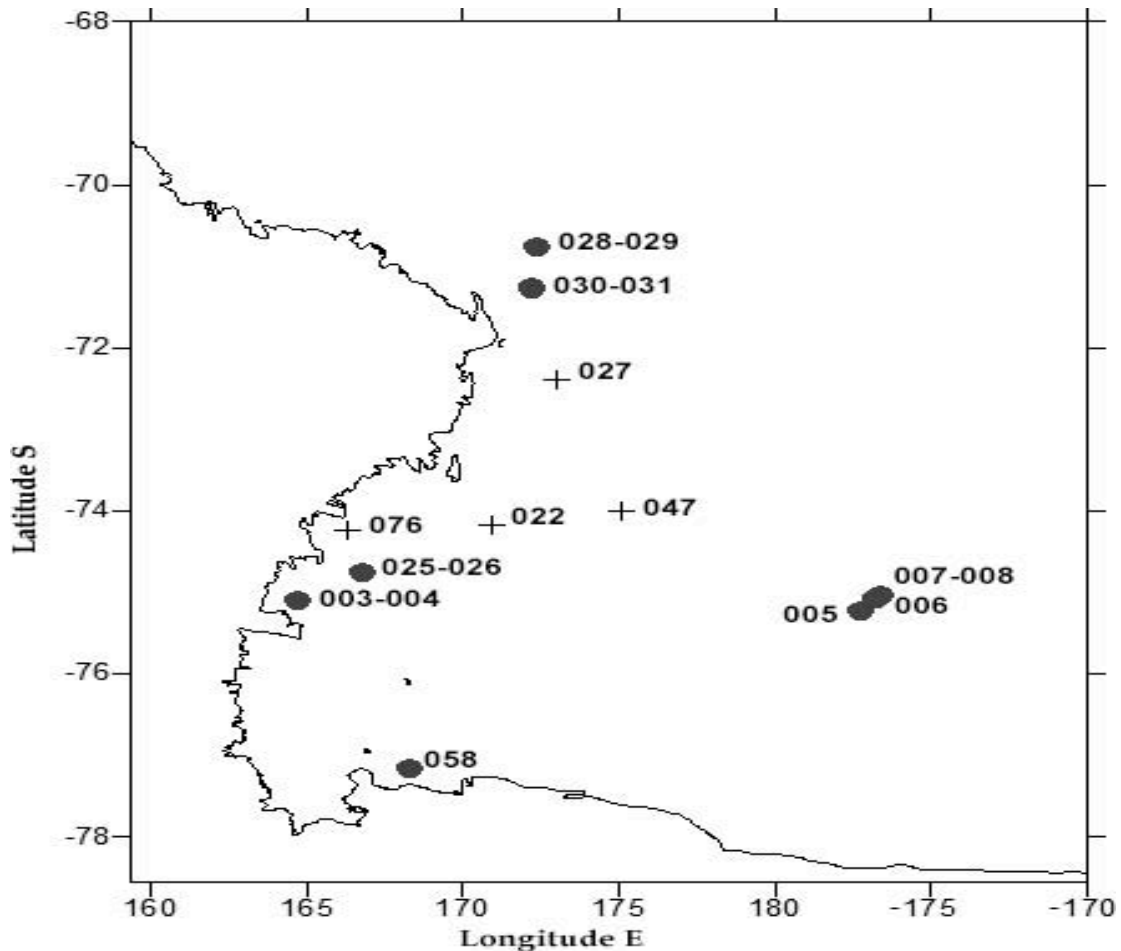
Fig. 5. Position of the sampled stations. Circles mark the stations where the experiments have been conducted. Crosses indicate the stations where the carbonate system has been characterized.

2.2   SAMPLING PROCEDURE

Hydrological characteristic and water sampling were performed using a rosette equipped with a SBE 9 CTD and 12L Niskin bottles (Fig. 6).

CTD stands for conductivity, temperature, and depth, and refers to a package of electronic instruments that measure these properties. Conductivity is a measure of how well a solution conducts electricity and is directly related to salinity, which is the concentration of salt and other inorganic compounds in seawater. Salinity is one of the most basic measurements used by ocean scientists. When combined with temperature data, salinity measurements can be used to determine seawater density, which is a primary driving force for major ocean currents. Often, CTDs are attached to a much larger metal frame called a rosette, which may hold water sampling bottles that are used

15

to collect water at different depths, as well as other sensors that can measure additional physical or chemical properties.
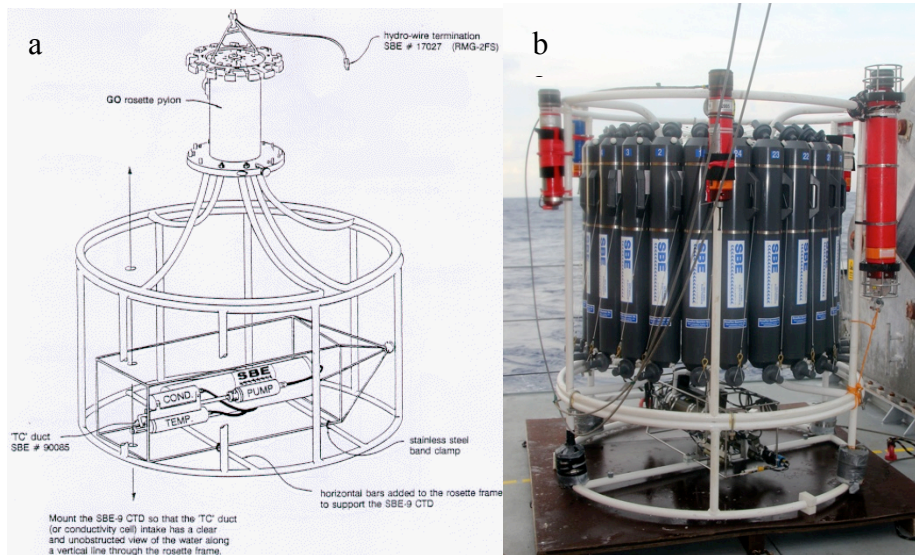
Fig. 6. SBE 9 CTD sensors (a), rosette with 12l Niskin bottles (b)

Thanks to CTD sensors profile, it was possible to collect data useful to identify characteristics of water masses at 5 - 11 different depths.

We identified 17 sampling stations where were gathered data on temperature, salinity, density, dissolved Oxygen, nutrients, carbonate system, dissolved organic C, N and P, particulate organic C and N. In 13 of the 17 stations, experiments of predation of nano- on picoplankton were performed (Tab. 2). For the estimation of the abundance of pico- and nanoplankton, 200 ml of seawater were sampled, subsequently conserved in 2% buffered formaldehyde, stored in a cold room (4°C) maintained in the dark. Samples were processed, at home laboratory, follow the Porter and Feig (1980) protocol and counted with a 100x oil immersion objective using an Olympus BX60 F5 epifluorescence microscope equipped with a 100 W high – pressure mercury burner (HPO 100 W/2).

	Depth(m)	
St. 3-4	<u>1066</u>, 1000, 900, 800, 600, 500	<u>700</u>, 400, 100, sup
St. 5	495, <u>410</u>, 300, 240, 170, sup	
St. 6	<u>563</u>, 370, 320, 180, sup	
St. 7-8	<u>1072</u>, 1000, 800, 700, 600	<u>1066</u>, 400, 300, 100, sup
St. 25-26	<u>957</u>, 900, 800, 600, 500	<u>700</u>, 400, 200, 60, sup
St. 28-29	<u>1743</u>, 1600, 1400, 1200, 1000	800, 600, <u>450</u>, 150, sup
St. 30-31	<u>1401</u>, 1200, 1000, 800, 600	400, 300, <u>200</u>, 50, sup
St. 58	<u>899</u>, 800, 650, 400, 300, 200, 60, sup	
St. 76	922, 700, 550, 300,135, 55, 18, sup	

Tab. 2. Stations and depth,s the double stations indicates the same place but 2 different hydrological casts, the predation experiments were done at underline depths.

2.3 DILUTION METHOD: THEORETICAL CONSIDERATION

It is possible to identify three main technicques to estimate the predation on prokaryotes :

a) Uses of tracers as radioisotopes (^{14}C, ^{3}H) or fluorescent colorants able to identify bacterial cells in to the vacuole and cytoplasm of bacteriovorus. This method is characterized by short incubation time, but the tracer could be lost during the fixation process and a selective predation towards marked particles can happen.

b) Manipulations based on prey and predator encounter. With this methods it is possible to obtain the ingestion rate of the entire community and it consists of different phases as dimensional fractioning and the dilution of microbial populations. Incubation time should be quite long to allow a significant variation of the organisms. It is possible to estimate the variation of the microbial population only by counting, organisms, before and after the incubation.

c) Considering the prey activity of bacterivorus by examination of digestion enzymatic activity or digestive vacuole amplitude or identify tracers as fluorescently labelled bacteria in the vacuole of bacteriovorus (FLB).

Among the different approaches employed in determining the grazing impacts, the dilution method is the most broadly used in plankton ecology, for this reason, in this study,we adopted it.

The dilution method is, nowadays, considered as a standard protocol (Dolan et al., 2000), it was first set by Landry and Hassett (1982) and, in second time, modify by Landry *et al.,* (1995) and Gallegos (1989).

Dilution grazing experiments were applied to a large variety of marine and estuarine systems ranging from estuaries and coastal areas to open ocean waters (Bec *et al*., 2005; Berninger and Wickham, 2005; Collos *et al*., 2005; Fileman and Leakey, 2005; Garces *et al*., 2005; Jochem *et al*., 2005; Leising *et al*., 2005; Strzepek *et al*., 2005; Troussellier *et al*., 2005; Fonda Umani *et al*., 2005; Yokokawa and Nagata, 2005). This procedure, originally estimated the microzooplankton predation upon phytoplankton in a very simple way, by analysing changes in chl *a* concentration, without any manipulation of the organisms, but subsequently adapted to estimate the predation of nanoplankton on picoplankton.

The dilution approach relies on the reduction of encountering rates between prey and their grazers (Gallegos, 1989). This technique allows assessing the instantaneous factor of prey mortality due to predation (g) and the instantaneous factor of growth of the prey (k). The protocol consisting in the dilution of different seawater samples containing prey and predators, with the same seawater without any organism (filtered onto 0.22 μm pore size millipore filters), to reduce the chance for a predator to met a prey.

The proceeding theoretical development involves three restrictive assumptions:

1) The growth of individual prey is not directly affected by the presence or absence of other prey. The implication of this assumption is that a reduction in the density of cells in natural seawater will not, directly cause a change in the growth rate of remaining cells. To satisfy this assumption, dissolved nutrients must remains non-limiting, or equally limiting, to growth at all dilutions during the experimental incubations;

the growth of individual prey is exponential.

2) The clearance rate of individual consumer is assumed to be constant at all dilutions, therefore microzooplankton community does not vary during incubation (Evans and Paranjape, 1992).

3) The probability of a prey being consumed is a direct function of the rate of encounter of consumers with prey. This implies that consumers are not food-satiated at natural prey densities and that the number of prey ingested by a given consumer is linearly related to prey density.

Change in the density of a prey biomass (C), over a period of time t can be represented appropriately by the following exponential equation, based on Landry and Hassett (1982) protocol (Landry, 1993):

$$C_t = C_0\, e^{\,(k-g)t} \quad \text{or} \quad (1/t)\ln(C_t/\, C_0) = k-g$$

Where:

C_0 = the concentration of the prey (or total biomass) at the beginning of the experiment

C_t = the concentration of the prey (or total biomass) at the end of the incubation (time t)

k = the instantaneous coefficient of population growth

g = the instantaneous coefficient of grazing mortality

t = the incubation time

From the first postulate, the instantaneous coefficient of population growth k is not influenced by the dilution series, it remains constant during incubation; the instantaneous coefficient of grazing mortality g in accordance with the third postulate is proportional to the consumers and prey density. Since k is constant and g is proportional to the dilution series, the equation with two unknown k and g may be graphically solved from the regression of apparent growth against dilution factor: k is the intercept of the regression line on the Y - axis while g is the slope of the regression line (Fig. 7).
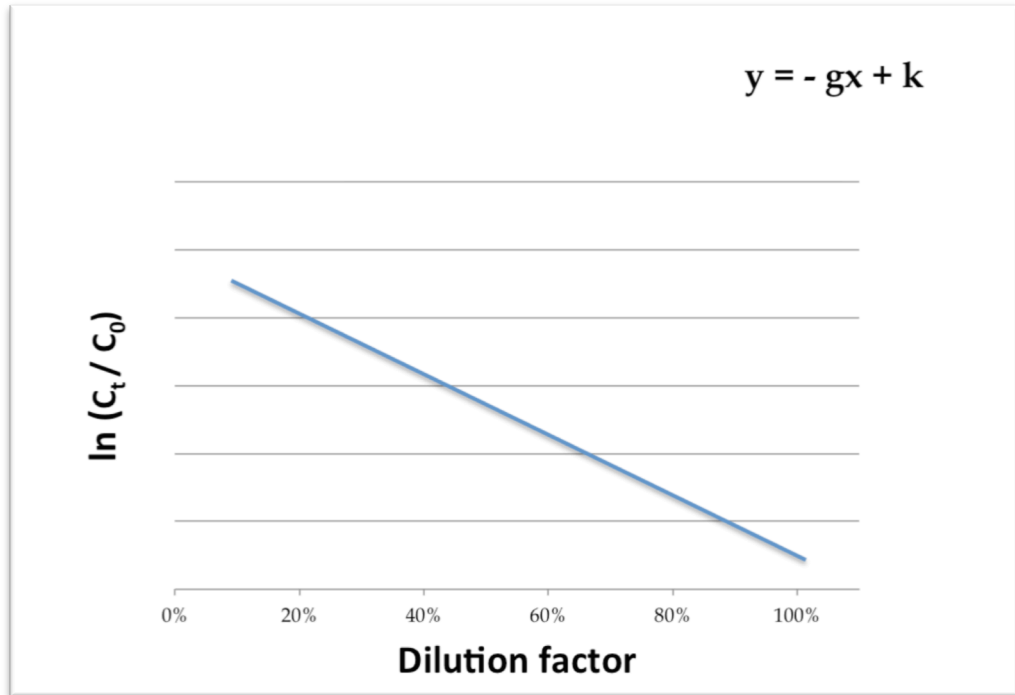
Fig. 7. Graphic representation of the linear regression model. The dilution factors are reported on the x-axis, while the apparent growth factor

The parameters can be calculated once obtained C_0 and C_t, the time is usually one day. With these values, it is possible to derive other parameters in order to evaluate the carbon flow during the experiment:

- C_m = The average concentration of the prey during the experiment expressed as $\mu g\ C\ L^{-1}\ d^{-1}$, and calculated with the equation derived by Calbet and Landry (2004):

$$C_m =\ C_0\,(e^{\,(k\text{-}g)_t} - 1)\,/(k - g)^t$$

- I = The ingestion rate, expressed as $\mu g\ C\ L^{-1}\ d^{-1}$, is intended as the amount of prey killed by predators in the t-time unit and in the experimental volume; it is calculated with the equation taken by Landry and Hassett (1982) and based on Frost (1972):

$$I = g * C_m$$

- P_p = The potential production , expressed as $\mu g\ C\ L^{-1}\ d^{-1}$, that is the

biomass which the prey would produce without predators; it is calculated
with the:

$$P_p = (C_0 * e^{k \times t}) - C_0$$

- P_R = The real production, expressed as µg C L^{-1} d^{-1}, that is the biomass
  produced by the prey with predators; it is calculated with the equation
  taken by Landry and Hassett (1982) and based on Frost (1972):

$$P_R = C_0 * e^{(k - g)t} - C_0$$

- %PP = The potential production removed by grazing is expressed as
  percentage and it is calculated with the equation:

$$\%PP = [(Pp-Pr)/Pp]*100$$

- %SP = The initial standing stock removed by grazing is expressed as
  percentage and it is calculated with the equation:

$$\%SP = [(Pp-Pr)/Pr+C0)]*100$$

2.4 DILUTION EXPERIMENTS

At 13 stations at different depths 20 liters of water were collected to assess the
predation of the heterotrophic nanoplankton on the picoplanktonic community. In order
to eliminate any possible organisms larger than the nanoplankton fraction, immediately
after collection, natural assemblages were gently poured through a nylon sieve with a
pore size of 200 µm on board and than filtered again in laboratory on a 10 µm net.

Two identical sets of four dilutions were made in the following proportions:
100%, 80%, 50 % e 10%; then for each dilution, three replicates were set up in 500 mL
bottles (each sets of dilutions has 12 bottles).

The water used to dilute the samples was obtained from the same water filtered
on a 0.22µm pore size hydrophilic membrane with a peristaltic pump (PFTE Millipore),

in order to exclude all organisms. The first set of dilution (T_0) was immediately fixed with formaldehyde at 2% final concentration. The second set of dilution (T_{24}) were kept in the dark and at the *in situ* temperature in a refrigerator for 24 hours.

All samples were conserved within black plastic bottles, in the dark and at 4°C, until the laboratory analysis.

2.4.1 Nanoplankton growth: secondary production

Simultaneously to the dilution experiments the growth of the predator (nanoplankton) was also investigated. Secondary production is the biomass produced by consumers per volume unit and time ($\mu g \ C \ L^{-1}d^{-1}$) and derived from the difference between the biomass average of nanoplankton calculated at T_{24} and T_0 only for not diluted samples (100%).

2.4.2 Quantitative analysis

The quantitative analysis of pico- nanoplankton at each sampling station for each depth, was carried out at the University of Trieste, in the laboratories of the Department of Life Science, under the supervision of the Prof. Serena Fonda Umani. During my PhD thesis, a number of 106 samples were analysed.

The analysis was carried out following a modification of the Porter and Feig (1980) method. This technique is based on the microbial cells staining with the fluorescent dye DAPI.

2.4.2.1 *Staining and filtration*

Samples were stained through D.A.P.I. - Sigma (4'6 – diamidino – 2 – phenylindole is a fluorescent stain that binds strongly to A-T rich regions in DNA and can pass through an intact cell membrane and is used extensively in fluorescence microscopy) at $1\mu g \ mL^{-1}$ final concentration for at least 15 minutes in the dark to facilitate the formation of the complex DAPI-DNA. The DAPI-DNA complex, when excited at the wavelength of 365nm (UV) emits fluorescence in the blue region of the light spectrum, while the fluorescence bound specifically to organic molecules fluorescence in the yellow region, thus allowing to discriminate bacteria from dissolved and particulate detrital material. After stained, samples of picoplankton were filtered in

9 replicates while 3 replicates for nanoplankton were done. Picoplankton samples were filtered onto black 0.2 μm polycarbonate membrane filters (Whatman, 25 mm diameter) laid over pre-wetted 0.45 μm nitrocellulose backing filters (Millipore®, 25 mm diameter). Nanoplankton were filtered onto black 0.8 μm polycarbonate membrane filters (Whatman, 25 mm diameter) laid over pre-wetted 1.2 μm nitrocellulose backing filters (Millipore®, 25 mm diameter). Filtration was performed on a vacuum pump with a depression between 0.2 – 0.3 atm. The volume of the water samples used for the filtration varies in relation to the depth of the sample and the percentage of dilution. After filtration, filters were placed directly onto a microscope slide between two drops of immersion oil, covered with a covering slide and stored at -20°C until counting.

2.4.2.2 Count

Picoplankton and nanoplankton enumeration has been done with a 100x oil immersion objective using an Olympus BX60 F5 epifluorescence microscope equipped with a 100 W high – pressure mercury burner (HPO 100 W/2). Picoplankton heterotrophic cells counting consisted in enumerate the cells present on the ocular grid (Patterson) by moving randomly the filter, through the UV microscope filter (365 nm) and counting at least 200 cells.

The abundance of autotrophic picoplankton was determined by using the filter cube U-MWIG (Olympus Rhodamine, excitation 520-550nm, emission 580 nm long pass) because it allows the green light to excite the natural pigment, phycoerythrin. The phototrophic bacteria were recorded considering the whole field of view and counting at least 150 cells.

Nanoplanktonic cells were counted considering three size classes: 2-3, 3-5, >5 μm (Christaki *et al*., 2001) to assimilate each organisms to a sphere of the same diameter and then calculate the biovolume. Were counted at lest 200 individuals. Autotrophic and heterotrophic nanoflagellates cells were counted on the whole field of view.

The count of the phototrophic organisms has to be really fast because the fluorescents signal fades quickly. Cellular abundances derived from counts, were calculated merging two proportions in the following formula:

$$Cell / L = (N*S)/ (A*V)$$

Where:

- *N* is the medium value of cells counted per field of view.
- *S* is the filtration surface expressed in mm^2 (related to the filtration area of the columns, equal to 200.96mm^2).
- *A* is the area of the field of view used in the counts, expressed in mm^2 (respectively equal to 3.8x102 mm^2 for the whole field and 9.6x104 mm^2 for the Patterson area).
- *V* is the volume in liters of the filtered sample.

The cellular abundance was converted in biomass multiplying Cells L^{-1} of each different kind of microorganisms for their conversion factor. Picoplankton abundance is converted to carbon content by using the conversion factor of 10 fg C cell^{-1} (Reinthaler *et al*., 2006), for nanoplankton, spheres with diameter equal to the medium value of the dimensional class were used as proxy to calculate their biovolume, the biomass was obtained multiplying it for the conversion factor of 183 fg C μm^{-3} (Caron *et al*., 1995).

With these converted values it was possible to estimate: growth factor (intercept), grazing factor (slope), initial concentration of the prey, mean concentration of the prey during the experiment, ingestion rate, potential production, real production, potential production removed by grazing, initial standing stock removed by grazing.

2.4.3 Cluster analysis

Cluster analysis is sensitive to outliers. Outliers can represent truly aberrant observations that are not representative of the general population. Similarity is another important concept of cluster analysis. Similarity can be measured in variety of ways, but three methods dominate the application of cluster analysis: correlation measures, distance measures, and association measures. Each of the methods represents a particular perspective on similarity, dependent on both its objectives and type of data. Both the correlation and distance measures require metric data (Ilango *et al*., 2011). Our cluster analyses were computed using "Past" program (Hammer et al., 2001). For the cluster analysis we used the similarity index Bray-Curtis and the algorithm UPGMA (paired group).

3 RESULTS

3.1 ENVIRONMENTAL DATA

Thanks to the CTD it has been possible to assess the characteristics of water in all 17 sampling stations at each depth in the study area (which stretches between 70° 30 'and 77° 30' S and 164° 00'E and 175° 00 'long W) and associate the water masses of belonging. For the predation experiment 13 stations were identified with the following characteristics (Tab. 2):

	Depth (m)	Temperature [deg C]	Fluorescence [ug/l]	Salinity [PSU]	Potential temperature [deg C]	Density [kg/m^3]	Oxygen (mg/l)	Water masses
Staz.3	1066	-1,8854	0,0246	34,7739	-1,9173	28,0005	7,36172	**HSSW**
Staz.4	700	-1,9035	0,0086	34,7487	-1,9218	27,9802	7,54436	**HSSW**
Staz. 5	410	-1,9644	0,0103	34,6441	-1,9736	27,8964	7,33046	**ISW**
Staz. 6	563	-0,7779	0,0097	34,6273	-0,797	27,8432	6,47484	**CDW**
Staz. 7	1072	-1,7197	0,008	34,6642	-1,7531	27,9068	6,92164	**HSSW**
Staz. 8	1066	-1,7306	0,0131	34,6637	-1,7637	27,9067	6,93391	**HSSW**
Staz. 25	957	-1,8905	0,0098	34,7724	-1,9176	27,9994	7,51776	**HSSW**
Staz. 26	700	-1,902	0,0087	34,7564	-1,9203	27,9864	7,63088	**HSSW**
Staz. 28	1743	-0,9222	0,0851	34,6999	0,3441	27,845	4,98384	**AABW**
Staz. 29	450	0,7063	0,0041	34,7079	1,1187	27,8027	4,7713	**CDW**
Staz. 30	1401	0,2554	0,008	34,6865	0,1856	27,8431	5,28706	**CDW**
Staz. 31	200	0,3809	0,0085	34,5844	0,3728	27,7501	5,40283	**CDW**
Staz. 58	899	-1,8813	0,0092	34,732	-1,9065	27,9662	7,166	**HSSW**

Tab. 2. CTD parameters and the water masses related to the 13 predation experiments

The surface temperature was >0°C at stations 4, 5, 26, 29, 58, 76. The lowest temperature corresponded to the station number 6 with -0,99°C while the highest was registered on station number 4 with 1,47°C. In the station 4-3 and 26-25 near Terra Nova Bay surface temperature of 1,47°C and 1.45°C were registered, respectively, in agreement with Fonda Umani *et al*., (1998). The salinity profiles, in the coastal areas showed a growing trend from 34.1 to 34.7 approximately for the first 200m and then salinity remained constant till the bottom with some exceptions as st. 76 were the surface salinity was about 33 and station 3-4 and 25-26 where salinity reach 34.77 at the depth of 1000m. Prevailing surface thermal processes due to both atmospheric and

orographic phenomena, which can maintain the polynya over winter, affect this area. Offshore stations presented a surface salinity range from 34.1 to 34.3 with an increase of salinity with depth but never exceeding 34.7 except at st. 6 at the depth of 370m where the value of salinity was 34.72. Surface temperature, at offshore stations, was characterized by value >0°C only at the st.5 (0.28°C), instead negative value of temperature were found at st. 8 (- 0.3°C) and st. 6 (-1,0°C). Eastward, dilution processes due to ice melting affected the offshore surface water consequently, the salinity was <34.6.

3.2 DILUTION EXPERIMENTS

The accuracy of dilution analysis of initial samples (T_0) has been verified for all stations. For all samples a decrease in abundance related to their dilution factor was observed (Fig. 8). As reported in Table 3, the *p*-values are largely statistically significant (p < 0.001) and the increasing of dilution corresponds to an effective dilution of the organisms.

3.2.1 Picoplankton

Comparing picoplankton cellular abundance at T_0 and T_{24} it was possible to estimate for each dilution level the apparent growth rate. Observing the negative slop of the straight in the (Fig. 9), it has been found a significant correlation between the apparent growth rate and the dilution factor at stations 3, 4, 6, 7, 29, 31 (correlated with a grazing pressure) while no correlation was found at stations 5, 8, 25, 26, 28, 30, 58.

	m	b	r	p-value
S.t 3	$3,61 \times 10^7$	$2,48 \times 10^7$	0,94	$3,65 \times 10^{-7}$
S.t 4	6×10^7	2×10^6	0,85	$1,41 \times 10^{-4}$
S.t 5	3×10^7	1×10^7	0,97	$6,53 \times 10^{-9}$
S.t 6	4×10^7	$8,2 \times 10^5$	0,92	$4,18 \times 10^{-6}$
S.t 7	3×10^7	4×10^6	0,97	$1,35 \times 10^{-8}$
S.t 8	3×10^7	6×10^6	0,95	$2,92 \times 10^{-7}$
S.t 25	8×10^7	2×10^7	0,94	5×10^{-7}
S.t 26	2×10^7	1×10^7	0,9	$8,7 \times 10^{-8}$
S.t 28	2×10^7	1×10^7	0,78	$9,45 \times 10^{-4}$
S.t 29	4×10^7	9×10^6	0,92	$4,44 \times 10^{-6}$
S.t 30	3×10^7	6×10^6	0,94	$4,1 \times 10^{-7}$
S.t 31	3×10^7	5×10^6	0,95	$1,41 \times 10^{-7}$
t 58	7×10^7	2×10^7	0,98	$9,48 \times 10^{-10}$

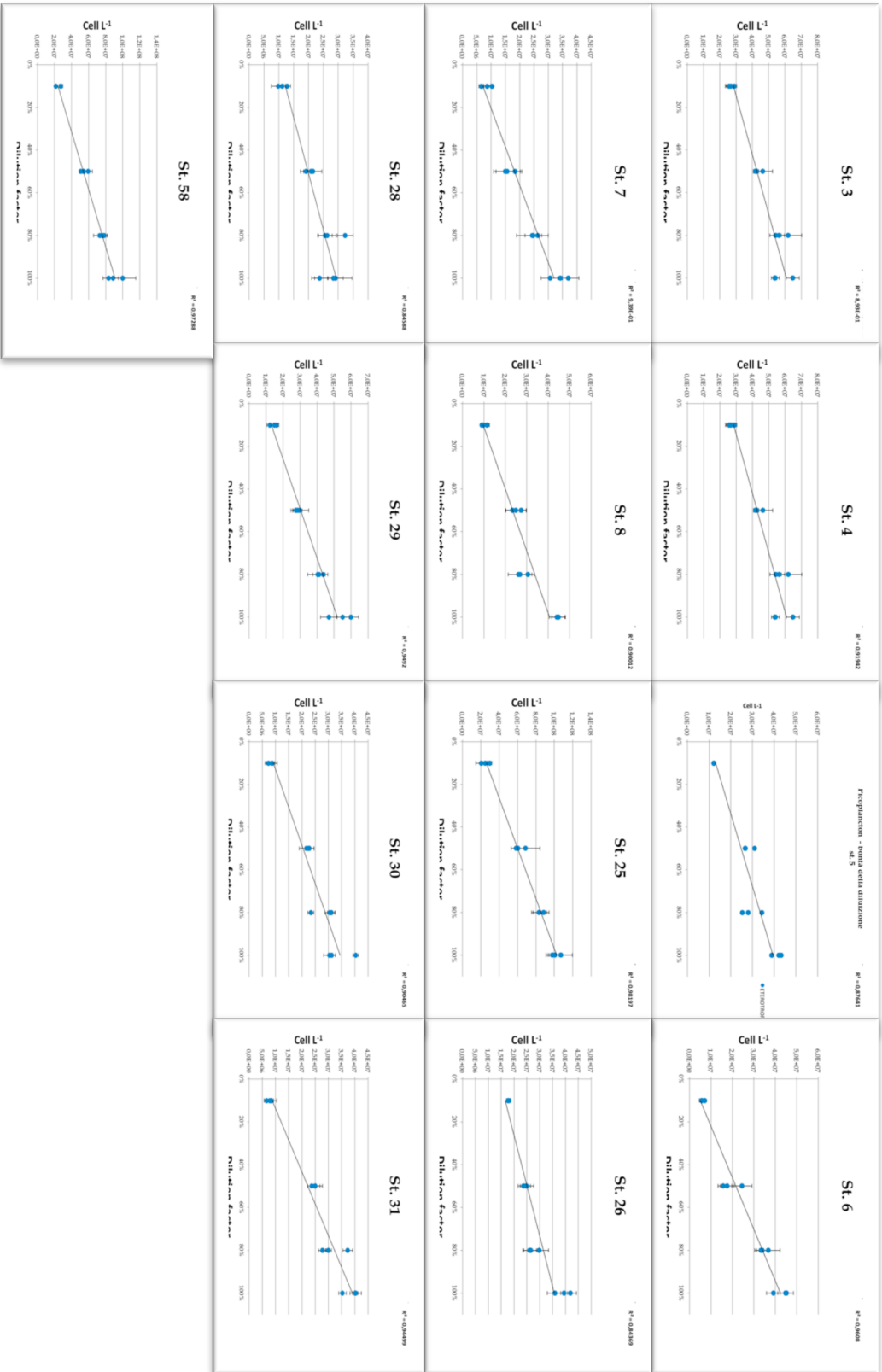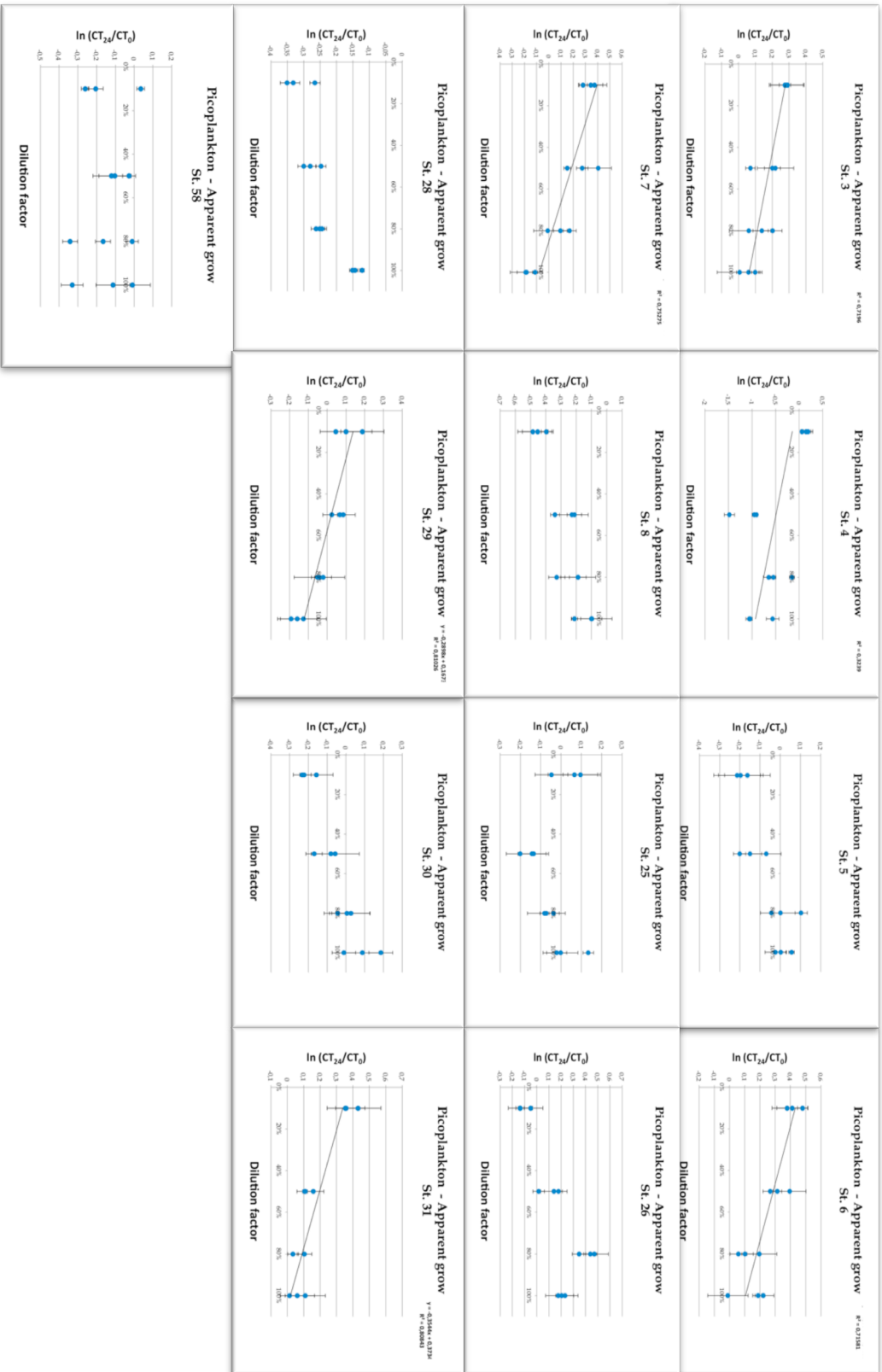**Tab. 3**. Synthesis of the parameters extrapolated from each dilutions experiment.

Fig. 8. Accuracy of dilutions for all the stations

Fig. 9. Apparent grow rate. Significant correlation is found on stations, 4, 6, 7, 29, 31 characterized by the negative slop of the slight.

Considering only stations were the correlation was significant, it was possible to calculate other coefficients that allow to understand the effect of the grazing (see Table 3);

At the four Cape Adare stations the number 29 and 31 presented a positive correlation. Station 29 present r = 0.91 and p < 0.001, instantaneous coefficient of population growth k = 0.16 and an instantaneous coefficient of grazing mortality of g = 0.27 determine an ingestion rate I = 0.14 µg C $L^{-1}d^{-1}$. Station 31 presented r = 0.86 and p < 0.001, instantaneous coefficient of population growth k = 0.39 and an instantaneous coefficient of grazing mortality of g = 0.34 determine an ingestion rate I = 0.14 µg C $L^{-1}d^{-1}$.

Stations 3 and 4 (Terranova Bay) were characterized respectively by r = 0.85 and r = 0.72 with p < 0.001. At station 3 instantaneous coefficient of population growth k = 0.31 and an instantaneous coefficient of grazing mortality of g = 0.24 determine an ingestion rate I = 0.15 µg C $L^{-1}d^{-1}$. At the station 4 it was evaluated a k of 0.08, g = 0.95 with an ingestion rate of I = 0.42 µg C $L^{-1}d^{-1}$

Among the off shore stations 5,6,7,8, only stations 6 (r = 0.83; p < 0.001) and 7 (r = 0.86; p < 0.001) presented a positive correlation between the apparent growth rate and the dilution factor. The st.6 showed a k = 0.47 a g = 0.36 and I = 0.16 µg C $L^{-1}d^{-1}$ while st. 7 was characterized by a k = 0.45 a g = 0.52 and I = 0.17 µg C $L^{-1}d^{-1}$.

St.	g	k	C_0 (µg C $L^{-1}d^{-1}$)	C_m (µg C L^{-1})	I (µg C $L^{-1}d^{-1}$)	P_P (µg C $L^{-1}d^{-1}$)	P_R (µg C $L^{-1}d^{-1}$)
3	0,24	0,31	0,57	0,59	0,15	0,21	0,04
4	0,95	0,08	0,67	0,45	0,42	0,05	-0,39
6	0,36	0,47	0,43	0,46	0,16	0,26	0,05
7	0,52	0,45	0,34	0,33	0,17	0,19	-0,02
29	0,27	0,16	0,54	0,51	0,14	0,10	-0,05
31	0,34	0,39	0,39	0,39	0,14	0,18	0,02

Tab. 3. Overview of the results of the dilution experiment. k= the coefficient of bacteria population growth, g = the coefficient of grazing mortality, C0 = the concentration of bacteria (or total biomass) at the beginning of the experiment, Cm = the average concentration of the prey during incubation time, I = ingestion rate, PP = the potential production, PR = the real production.

Comparing abundances at T_0 and T_{24} at 100% of dilution, it was possible to observe a slight increase, of the cells abundance, at T_{24} for st. 3, 6, 31, a drastic

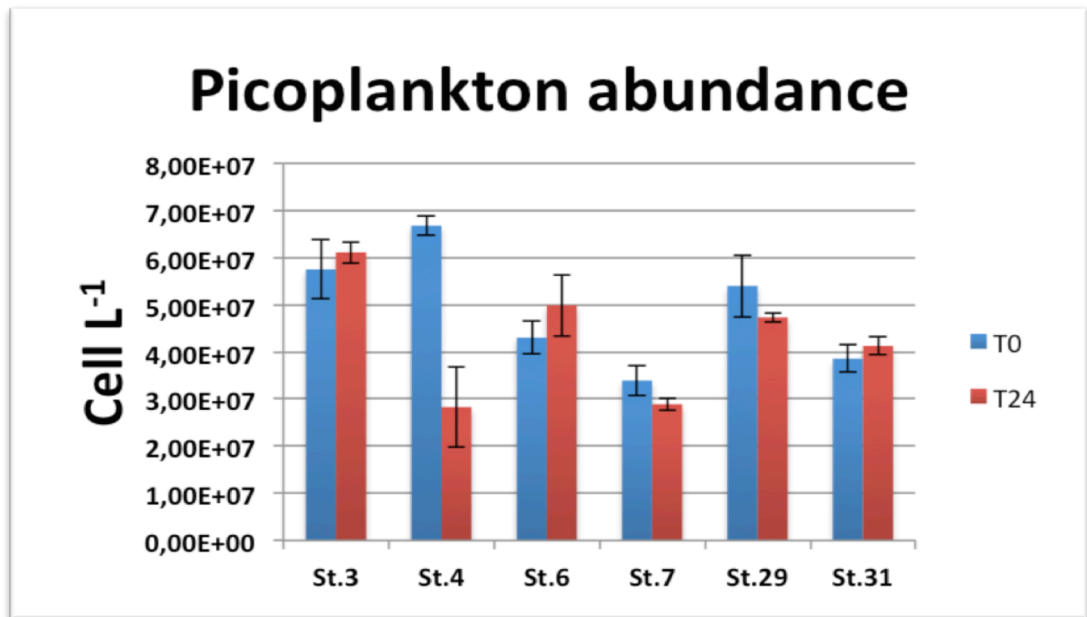reduction at st. 4 and a slight reduction at st.7 and 29 (Fig. 10).

**Fig. 10.** Abundance of picoplankton at T_0 and T_{24} at 100% of dilution.

At T_0, st. 7 and st. 4 presented, respectively, the lowest and the highest value of picoplankton. Picoplankton abundance ranged between 3.39×10^7 Cell L^{-1} and 6.68×10^7 Cell L^{-1} while biomass varied from 0.34 µg CL^{-1} and 0.67 µg CL^{-1}. After 24 hours (T_{24}), abundance ranged between 2.83×10^7 Cell L^{-1} (st. 4) and 6.11×10^7 Cell L^{-1} (st. 3) while biomass varied from 0.28 µg CL^{-1} (st. 4) and 0.61 µg CL^1 (st.3).

		St. 3	St. 4	St. 6	St. 7	St.29	St. 31
Cell L^{-1}	**T0**	5,75E+07	6,68E+07	4,30E+07	3,39E+07	5,40E+07	3,86E+07
	T24	6,11E+07	2,83E+07	4,99E+07	2,89E+07	4,73E+07	4,13E+07
µg CL^{-1}	**T0**	0,57	0,67	0,43	0,34	0,54	0,39
	T24	0,61	0,28	0,5	0,29	0,47	0,41

Tab. 4. Abundance and biomass at T_0 and T_{24}

Comparing the growth factor and the grazing factor of each stations (Fig. 11), it is easy to understand how st. 3, 6 and 31 stay up the median of the quadrant close to the

grow factor-axis, this means that the growth rate of prey overcame the grazing rate (the production of new cells is higher than grazing), conversely st. 4, 7 and 29 are located under the median near the grazing factor, meaning that the grazing pressure overcame the growth rate and in this case the picoplankton were top-down controlled by grazers. Median represents the situation of equilibrium in which the new cells pair the cells that die.
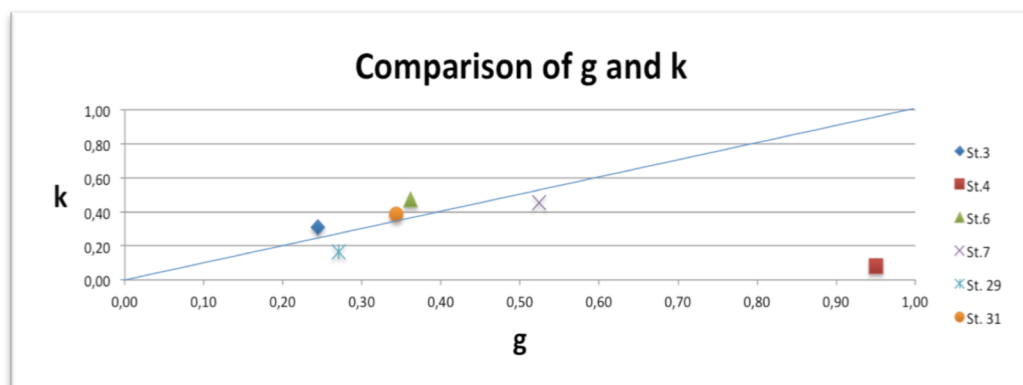

Fig. 11. Comparison graphic of the grazing factor (g) and the growth factor (k). The blue line represent the median of the quadrant, over it the growth overcame the grazing and vice versa below the line.

3.2.2 Nanoplankton

Nanoplankton abundance (Fig. 12 a,b) and biomass (Fig. 13 c.d) was estimated in 3 replicates at the beginning (T_0) and at the end of the experiment (T_{24}) using the 100% dilution (sea water not diluted) for each size class. Taking a more in depth analysis of nanoplankton size class, it is possible to make some considerations:

- The smallest size component (>3 μm) was predominant, followed by the intermediate (3-5 μm) and, at the end, the biggest cell size class (>5 μm). This is in agreement with Christaki et al. (2001) who claimed that the population of predators is numerically mainly composed by the smallest fraction, subsequently by the intermediate fraction and the biggest organism fraction at the last.

- The size class that give a major contribute in reduction from T_0 to T_{24} are cells with a diameter >5 μm followed by 3-5 μm. This is in agreement with the hypothesis on the fact that an organism with a large size requires higher metabolic needs compare to a small one therefore nanoplanktonic cells in the size of >5 μm are the first organisms to be affected by the reduction of prey abundance.
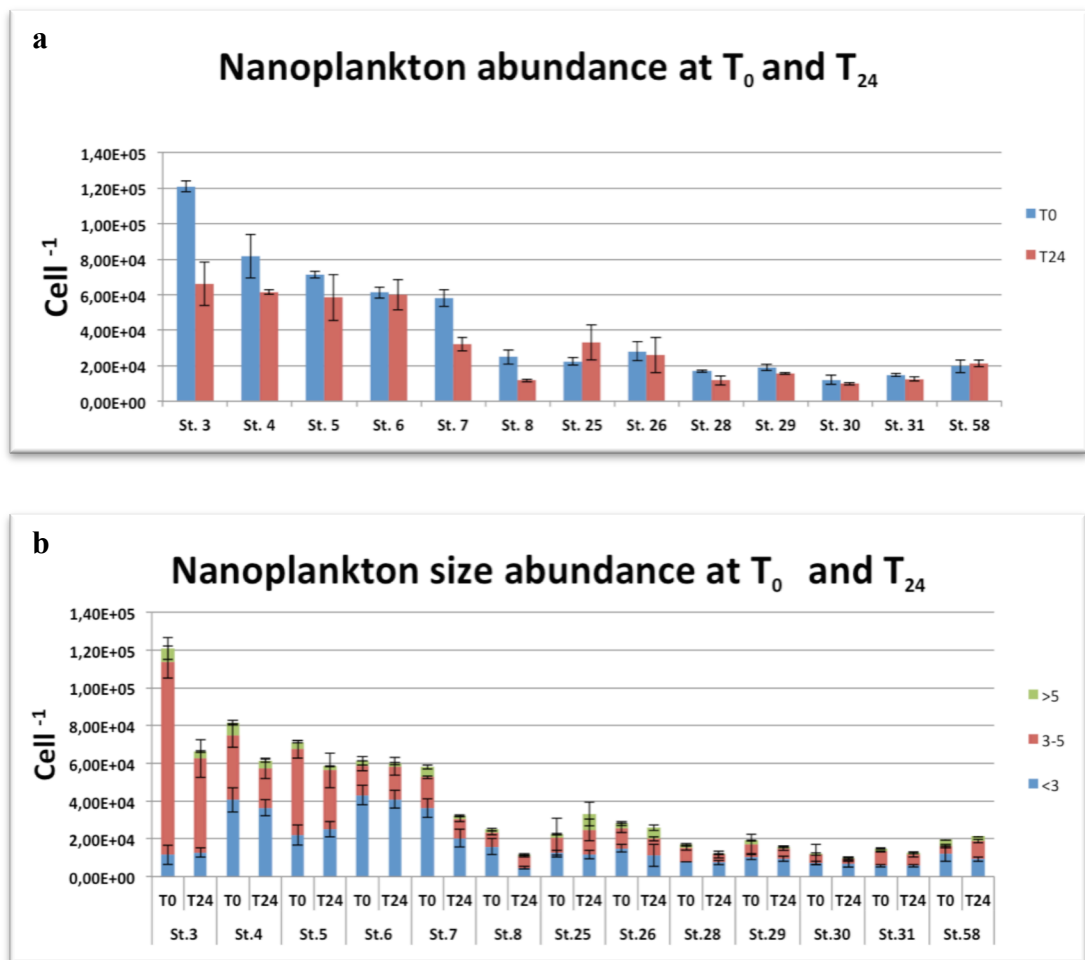
Fig. 12. Nanoplankton abundance. a) Total nanoplankton abundance, b) Nanoplankton size abundances

An increase in biomass, during the incubation period, denotes the hypothetical growth of the predator known as secondary production. A reduction of biomass is detected at stations 3, 4, 5, 7, 8, 28, no significant variation at stations 6, 26, 29, 30, 31, 58 while only station 25 presented an increase of the predators (Fig. 13 a).
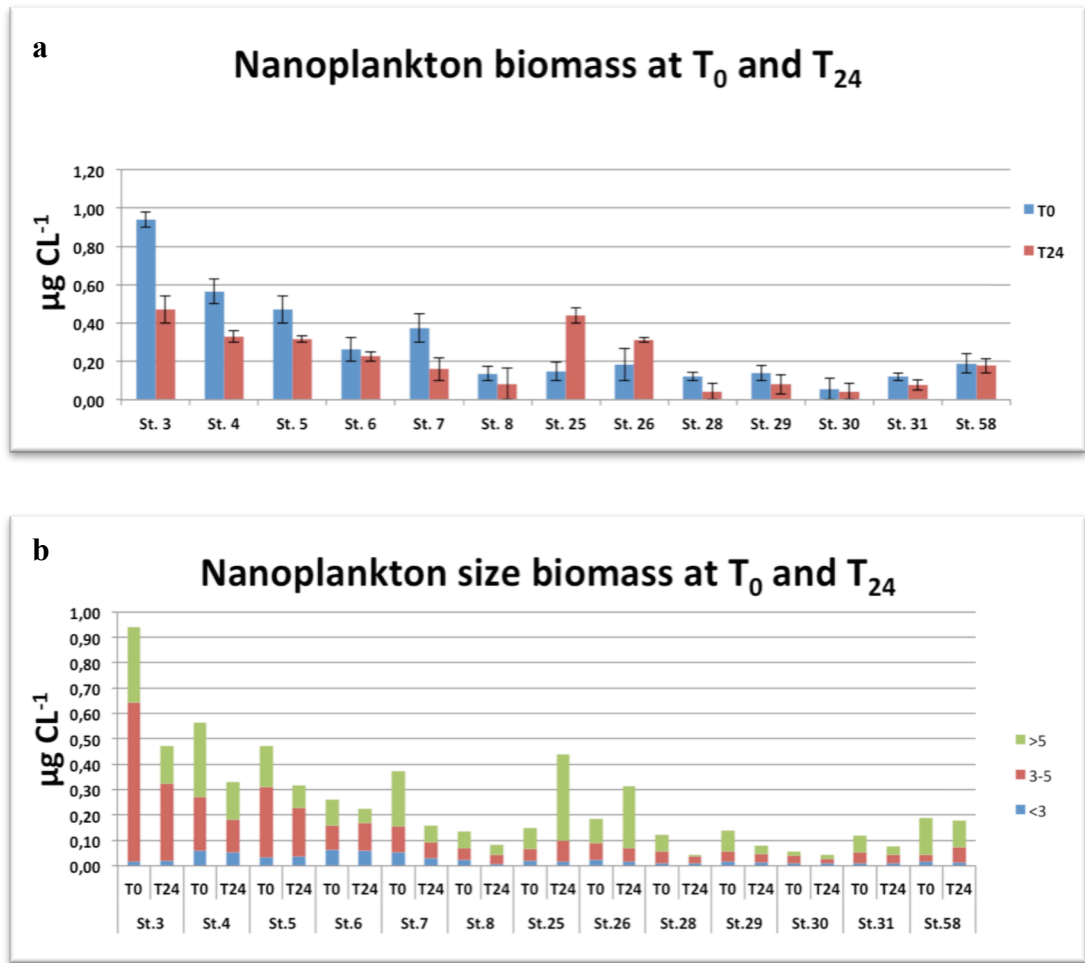
Fig. 13. Nanoplankton biomass. a) Total nanoplankton biomass, b) Nanoplankton size biomass

3.3 DISTRIBUTION ANALYSIS

The analysis of samples collected at different depths at different stations, allowed me to evaluate the total abundance and biomass of pico- nanoplankton and dimensional nanoplankton classes along the water column and its variation inside the different water masses.

3.3.1 Picoplankton

Putting in relations the depth of each station with the cellular abundance, it was possible to delineate the trend of the picoplankton variations (Fig. 14). Station 3-4 showed a decrease in abundance from the surface layer (with a maximum abundance value of $1,94 \times 10^8$ Cell L$^-$) to about 500 m. Below this depth the abundance showed a no linear trend until 1000m with a minimum abundance value of 5×10^7 Cell L^{-1} at

900m of depth and proceed with an increase at the bottom. Station 25-26, was characterized by the highest value at the surface ($7{,}1 \times 10^8$ Cell L^{-1}) followed by a strong reduction of abundance until depth of 400m were the abundance remained constant till 800m reaching the minimum of $5{,}29 \times 10^7$ Cell L^{-1} with a slight increase near 1000m. The abundance of station 58, presented an "S" profile with a value of $7{,}61 \times 10^8$ Cell L^{-1} at the surface while the minimum value was found at 800m ($5{,}44 \times 10^7$ Cell L^{-1}). The profile seems to increase after 900m. Station 76 showed a surface value of $9{,}44 \times 10^8$ Cell L^{-1} and after 500m of depth the abundance was quite constant till 922m with a value of $4{,}68 \times 10^7$ Cell L^{-1}. Stations 28-29 and 30-31, were characterized by a very similar abundance profile. Surface presented a value of $2{,}33 \times 10^8$ Cell L^{-1} at station 28-29 and $3{,}28 \times 10^8$ Cell L^{-1} at the 30-31 station. Passing the depth of 1000m, the abundance remained more or less constant, for all this stations, with a value of $2{,}33 \times 10^8$ Cell L^{-1}. Off-shore stations (5, 6, 7-8), shown a very similar "L" profile with an abundance at surface ranging between $2{,}19 \times 10^8$ Cell L^{-1} and $3{,}95 \times 10^8$ Cell L^{-1} and at depth of 550 - 600m abundance ranging from $4{,}71 \times 10^7$ Cell L^{-1} and $5{,}70 \times 10^8$ Cell L^{-1}. The highest value observed at the surface was $9{,}44 \times x10^8$ Cell L^{-1} at St. 76 followed by St. 25-26 and St. 58
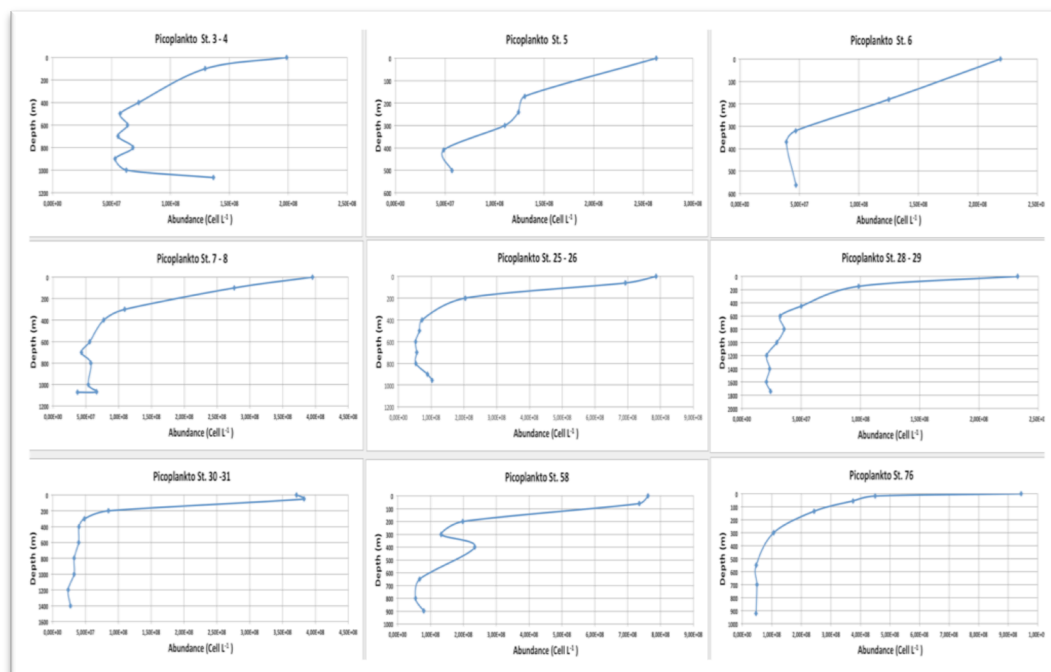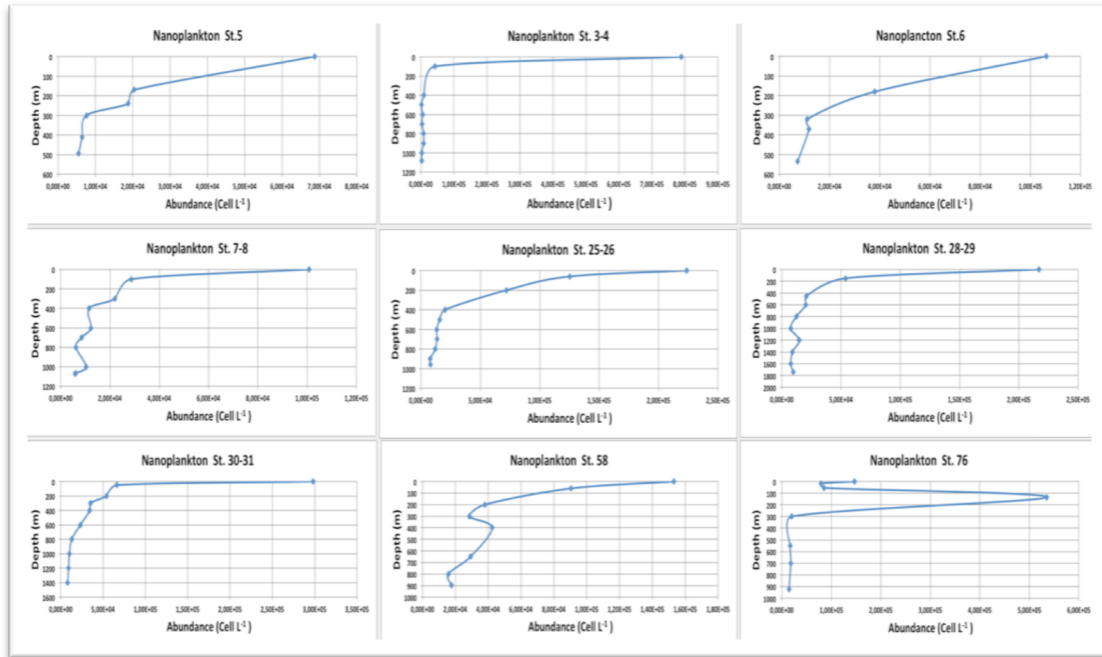

Fig. 14. Abundance profiles of the stations.

.

3.3.2 Nanoplankton

Nanoplankton evaluation was done considering the abundance and subsequently the biomass at each depth for every single station. Organisms were counted considering the size classes (2-3; 3-5; >5), and the trophic characteristics.

Nanoplankton total abundance profiles are shown in the Fig. 15. Stations show a similar abundance profile trend with some exceptions.


Fig. 15. Nanoplankton total abundance profile

Station 3-4 (near Drygalski Ice Tongue) is characterized by a surface value of $7,98 \times 10^5$ Cell L^{-1} followed by a reduction of approximately one order of magnitude at the depth of 100m proceeding with a zigzag trend till 1080m. The minimum value was observed at the depth of 500m ($2,10 \times 10^3$ Cell L^{-1}). In the Off shore stations (5, 6, 7-8) it is possible to distinguish the st. 5, with a surface value of $6,87 \times 10^4$ Cell L^{-1} and the minimum value ($5,50 \times 10^3$ Cell L^{-1}) at 500m of depth, station 6, with a surface value of $1,06 \times 10^5$ Cell L^{-1} and a minimum at 536m ($7,26 \times 10^3$ Cell L^{-1}) and finally station 7-8 that shows a surface abundance of $1,01 \times 10^5$ Cell L^{-1} with a minimum of $5,88 \times 10^3$ Cell L^{-1} at 1072m. Terranova Bay stations (25-26) are characterized by the highest value at the surface ($2,24 \times 10^5$ Cell L^{-1}) followed, below 400m, by a constant decreasing trend to the bottom. The lowest value is registered at 900m ($7,90 \times 10^3$ Cell L^{-1}).

Cape Adare stations (28-29, 30-31) show very similar values for the surface ($2,17 \times 10^5$ and $2,98 \times 10^5$ Cell L^{-1}) and for the bottom abundance at depth of 1400m ($8,93 \times 10^3$ and $8,10 \times 10^3$ Cell L^{-1}). Total abundance profile of Station 58 (near the Ross Island), show an "S" profile with a maximum value at the surface ($1,53 \times 10^5$ Cell L^{-1}), followed by a slight decrease until 300m and an increase culminating at 400m. The lowest abundance registered is visible at 800m, after this depth the trend seems to be increasing again.

Station 76 (near Wood Bay), slightly differs from other stations in the first 55m, in fact, the trend of the curve is irregular and the highest value of abundance is reached towards 135m and not at the surface. Below 135m, the curve is very similar to the other stations and the lowest value is observed at a depth of 922m ($1,45 \times 10^4$ Cell L^{-1}).

In the Fig. 16 and Fig. 17 is highlighted how abundance and the biomass of the hetero and autotrophic nanoplankton change from the surface to the bottom. All stations show a decrease in abundance from the surface layer to the bottom except station 58 that shows an increase in abundance at 400m on respect to 300 and 200m and 76 where at 135m we registered the highest value of abundance and biomass. Autotrophic organisms are concentrated, as usual, at the surface layers with some exception such as station 5 (240m), station 58 does not present any autotrophic organism from 60m to 200m but it is possible to observe autotrophic cells at 300m ($7,64 \times 10^3$ Cell L^{-1}) and station 76 with a very high value of autotrophic cells at 135m ($8,12 \times 10^5$ Cell L^{-1}). Comparing the abundance and biomass at surface layer (Fig. 18a; 18b) it is possible to make some considerations.

The highest value of abundance at the surface layer was found at station 3-4 ($4,74 \times 10^6$ Cell L^{-1}) while the lowest at station 5 ($4,29 \times 10^5$ Cell L^{-1}). The biomass distribution has a trend similar to that of abundance but the station 76 shows a high abundance related to autotrophic cells, this is due to an elevated number of organisms larger than 5 μm.
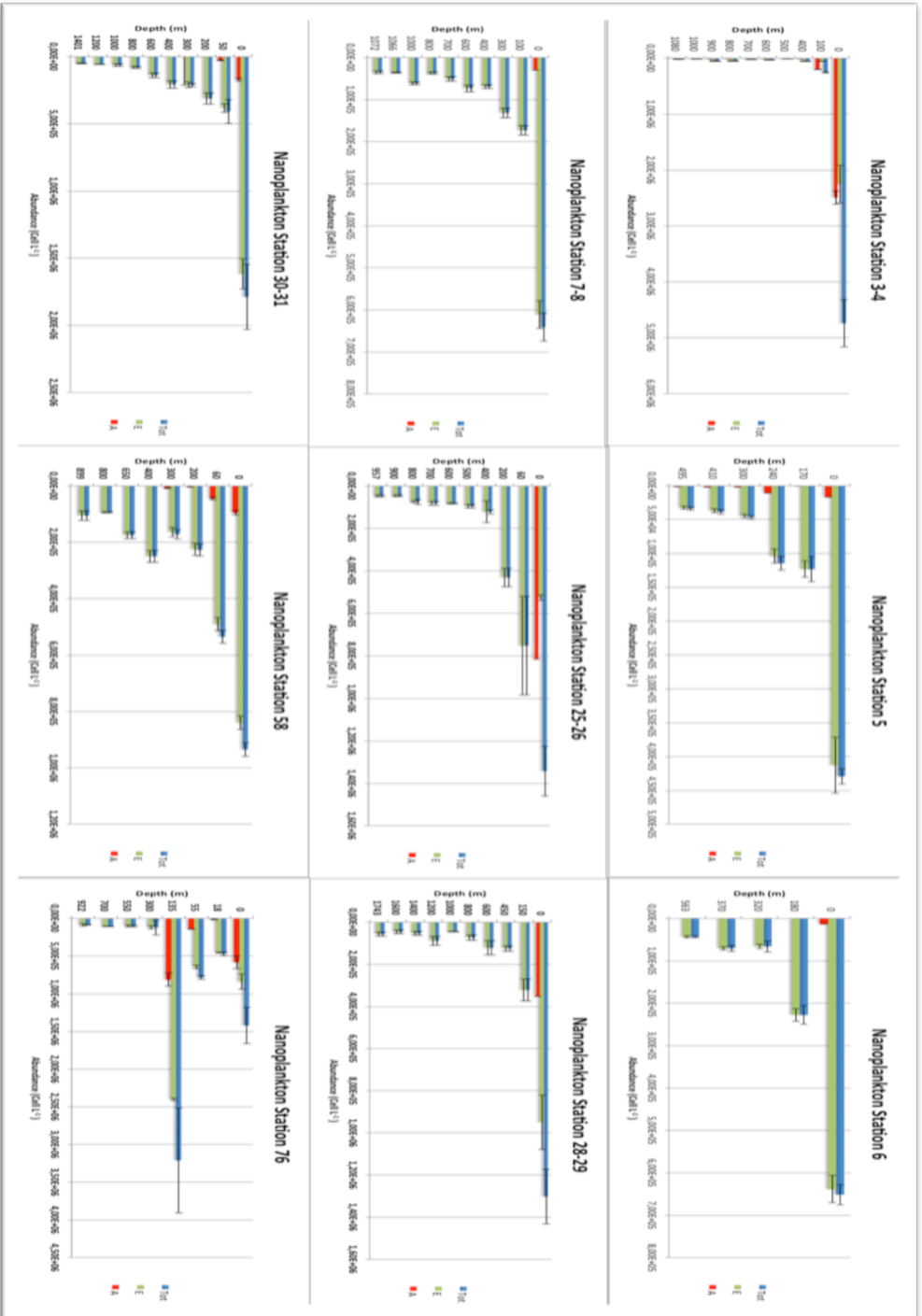
Fig. 16. Autotrophic and Heterotrophic Nanoplankton abundance. Blue column is referred to Total nanoplankton; red column is referred to Autotrophic nanoplankton; green column is referred to Heterotrophic nanoplankton
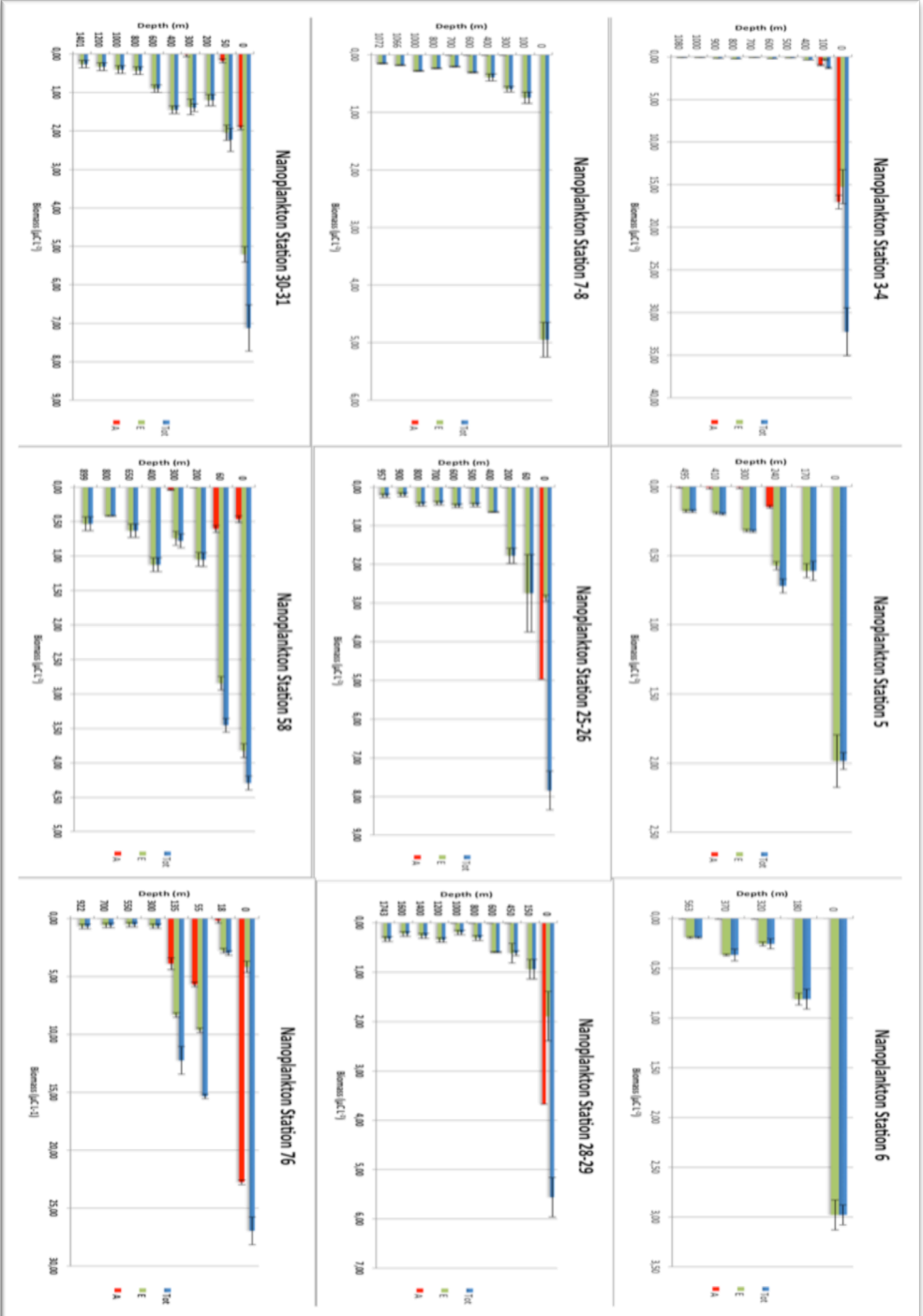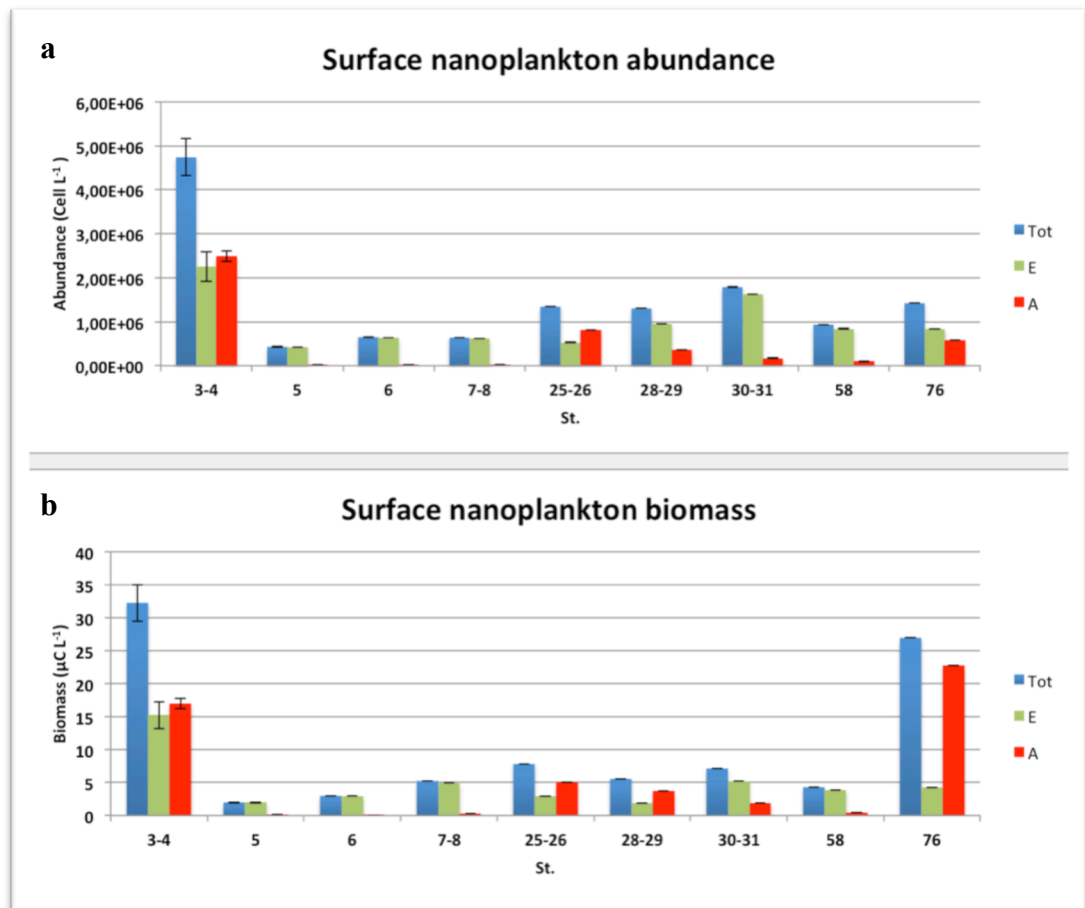
Fig. 17. Autotrophic and Heterotrophic Nanoplankton abundance. Blue column is referred to Total nanoplankton; red column is referred to Autotrophic nanoplankton; green column is referred to Heterotrophic nanoplankton

Fig. 18. Autotrophic and Heterotrophic Nanoplankton abundance at the surface layer. a) Nanoplankton abundance; b) Nanoplancton biomass.

Abundance dimensional classes graphs (Fig. 19) of all stations show higher values of 2-3 μm followed by 3-5 μm and in the end >5 μm. This is observed for both autotrophic and heterotrophic cells with the exception of stations 3-4 μm and 25-26 at surface layer where autotrophic cells in the class size of 3-5 μm are the highest of all depths. At station 76 we detected very high value of >5 μm class but only at the surface and only for the autotrophic cells. The trend of the biomass dimensional classes graph (Fig. 20) is very similar to the abundance one.
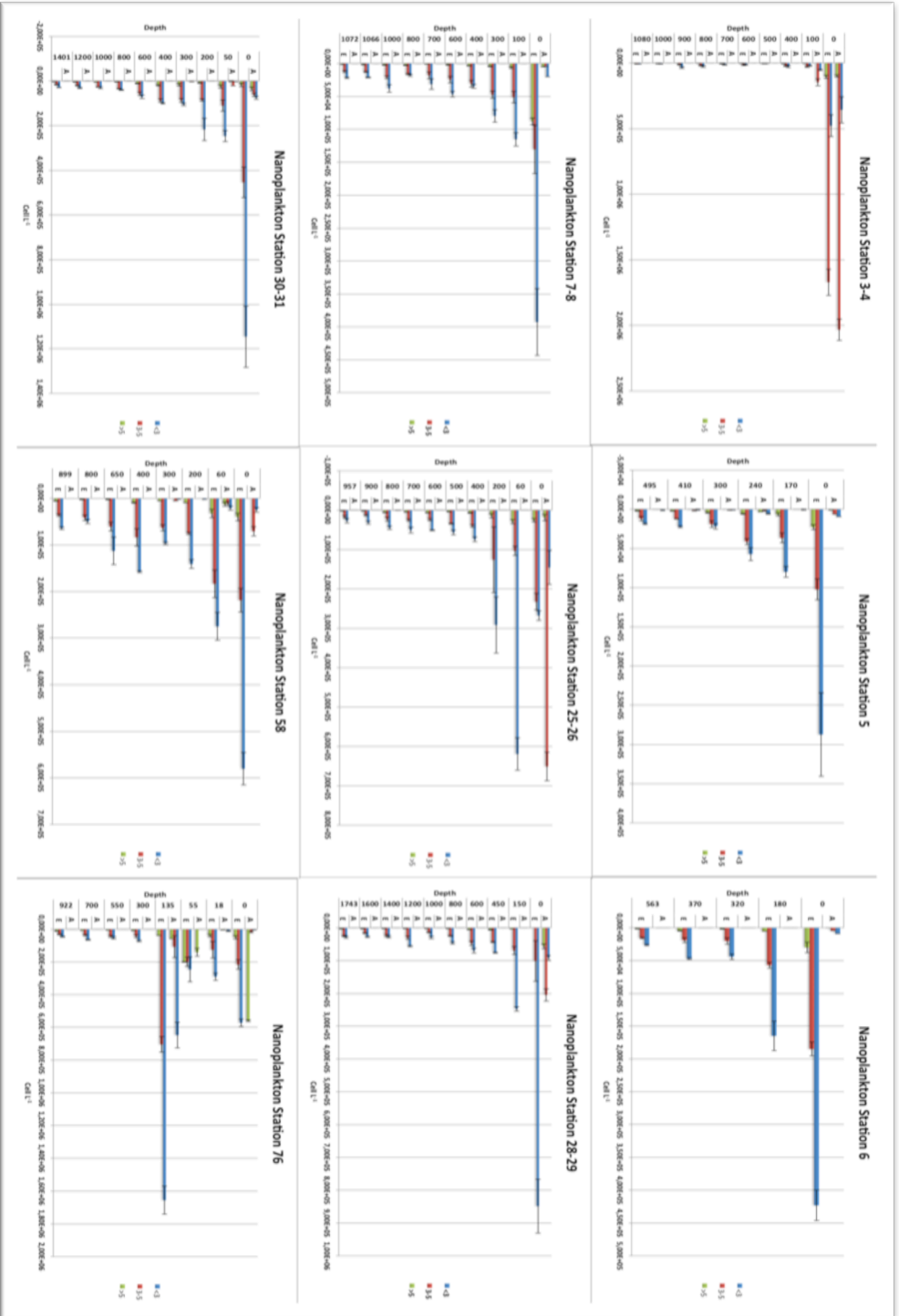
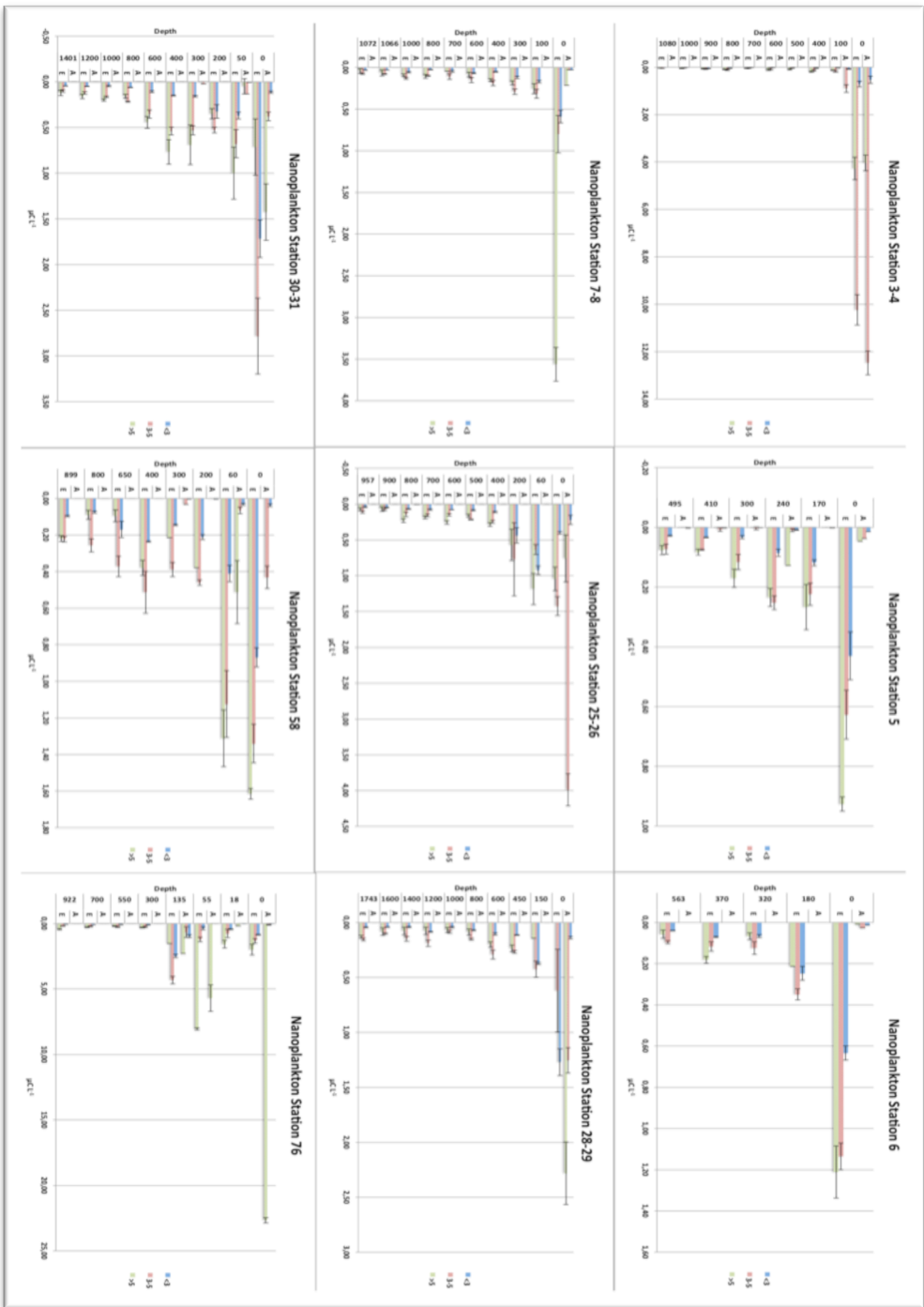**Fig. 19**. Autotrophic and Haeterotriphic Nanoplankton size class abundance

Fig. 20. Autotrophic and Haeterotriphic Nanoplankton size class biomass.

3.3.3 Quantitative analysis in different water masses

Thanks to CTD data it was possible to evaluate the water mass of reference for each depth of each station and with the cluster analysis to estabilish a possible correlation between the different water masses and the group of organisms analysed before.

In the Fig. 21 the different water masses found in the sampling area are represented. To better understanding the location of the samples in the water masses, samples were distinguished in 3 different layer. Surface layer (0m), intermediate layers (50- 900m) and bottom layer (900-1743m). All surface samples and someone of the intermediate layers in the range of 18 to 300m are included in the AASW. Four intermediate samples (from 170 to 300m) are included in the WW. In the CDW we registered many intermediate layer samples (depths ranging from 200 to 800m), and some bottom samples from 1000 to 1401m. In the HSSW we found 12 samples from 300 to 900m depth and 5 bottom samples (from 900 to 1066m). Less represented water masses in this experiments are the AABW (with just one samples belonging to the bottom layer at 1743m), and ISW with 2 samples at 410 and 495m.
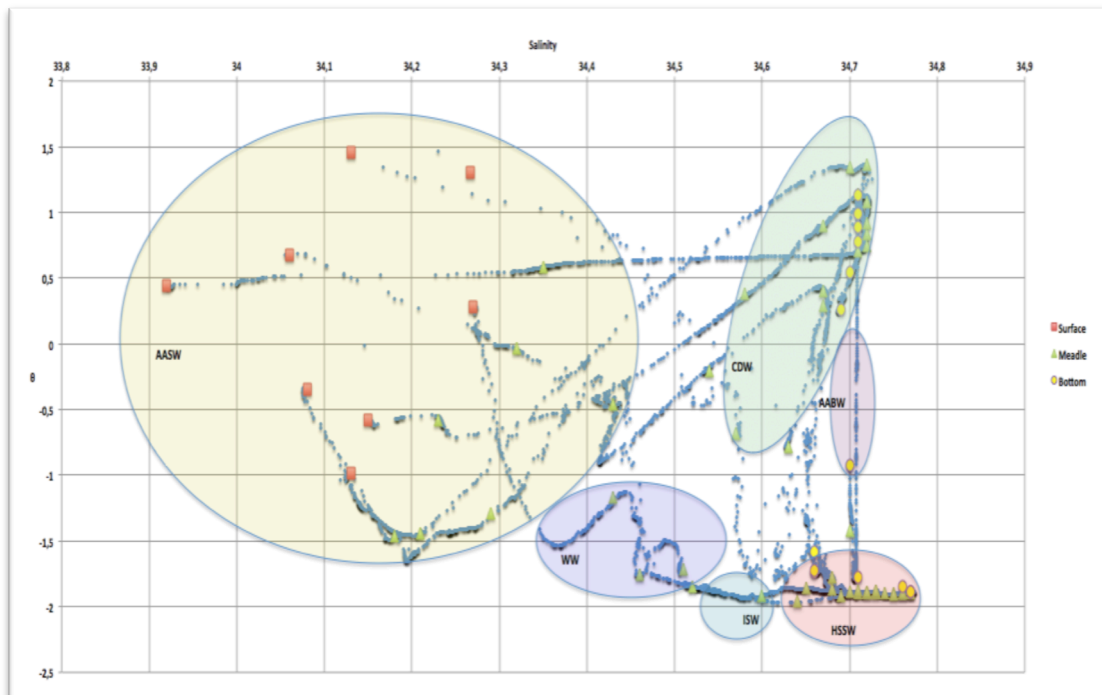
Fig. 21. Temperature-salinity diagram showing the characteristic water masses. All the depth of stations were divided in relation in 3 categories: surface layer(0), intermediate layer (50-900m) and bottom layer (900-1066m)

Clustar analysis applied on data of pico- and nanoplankton abundances generated the cluster shown in the Fig. 22 it is possible to observe a small group of station totally different from all the other grouped together, which belonged to AASW. Most of the rest of the groups do not clearly identify any water masses, only many samples (but not all) collected in CDW grouped together.
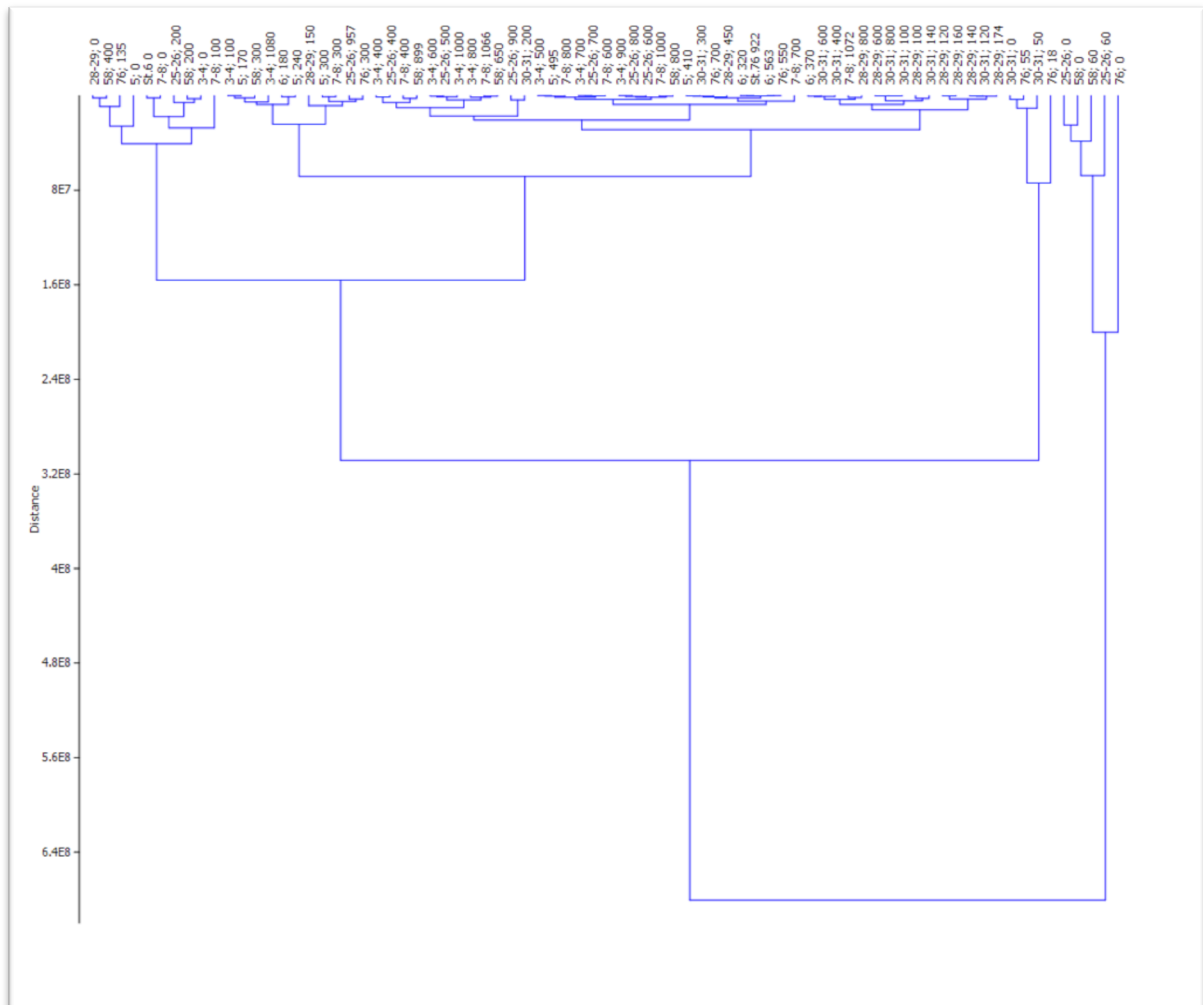
Fig. 22. Dendrogram obtained by applying cluster analysis on the matrix of quantitative data of pico – and nanoplankton of all samples

4 CONCLUSION

The water masses identified in the place of sampling, object of this study, are in agreement with previous research in the same area. The highest temperature at the surface was registered at st. 58 (0,67 °C near the Ross Shelf) and st. 3-4 (1,4 °C, near Terranova Bay), probably because they have been free from ice for a longer period.

Bacteria and phytoplankton being preyed by microzooplankton are responsible for much of the carbon transfer through the food web (Becquevort 1993; Burkill et al. 1995; Fonda Umani et al. 1998; 2010; Caron et al. 2000, Hall & Safi 2001, Landry et al. 2002).

It was possible to assess predation activity only in 6 out of 13 experiments, perhaps the incubation time of 24hr was not enough, and particularly at the lowest temperatures, for the predators to exert a significant impact on their prey. This hypothesis could be related to the cell metabolic reduction during the incubation period because of very cold environment. Del Giorgio et al., 1996 observed that high flagellates predation is shown mostly on prokaryotic cells with a high metabolic activity.

Three of the six samples, in the predation experiment, belong to the CDW while the other to the HSSW. But we were not able to detect any correlation between water masses and predation.

Although grazing rates were relatively high if compared to those measured in the meso – bathypelagic Mediterranean regions (Fonda Umani et a., 2010), only in 3 stations grazing rate exceeded growth rate, indicating an intense top – down control. Nevertheless of the few significant data on C fluxes we have to keep in mind that these are the first data for the Ross Sea interior, which will be useful for the eventual modelling exercises.

I analysed the vertical distribution of abundance (and biomass) of pico- and nanoplankton along the water column at 17 stations in the Ross Sea.

The most relevant result is the drastic decrease of both fractions from the surface toward the bottom, although not always perfectly linear. I did not observe any common trend for pico- and nanoplankton at any of the stations.

Indeed cluster analysis applied to the pico – and nanoplankton abundance matrix of all samples, put in evidence only few correlations between specific water masses and abundance distribution (only part of the CDW and ASW samples appeared strictly associated). It is evident that abundance data alone are not useful to identify specific samples associations, which can be highlighted only by using qualitative data that were not part of my research, but see Zoccarato et al., 2016, submitted.

Some research shown how the Antarctic ecosystem is highly dependant by several natural parameters, and small changes of one of this can bring deep change in biology. Plankton composition and biomass seasonal oscillations can be influenced not only by temperature changes but also by the length of the day (light availability), melting of pack ice, glacial melt waters and other significant sources (Brandini and Rebello 1994; Boyd 2002; Hewes 2009).

From the obtained results and consequent observations, it appears even more important to study not only the various components of the "microlitersphere", but also the ice conditions and their effect on the microbial presence in order to understand the Antarctic marine ecosystem. It would appear that each single size and metabolic component behaves in a particular way in relation to the biotic and abiotic environmental conditions.

More recent studies in some marine systems now suggest that the majority of particulate organic carbon instead of being exported may be remineralised with the aid of protist grazing and bacterial activity and hence may never reach the deep ocean (Buessler & Boyd 2009, Tanaka 2009, Sohrine et al. 2010). This in turn has important implications, especially if similar processes occur in the Southern Ocean waters, which are regarded as an important sink for atmospheric carbon (Sefi et al., 2012).

Bacteria and phytoplankton being preyed by microzooplankton are responsible for much of the carbon transfer through the food web (Becquevort 1993; Burkill et al. 1995; Fonda Umani et al. 1998; 2010; Caron et al. 2000, Hall & Safi 2001, Landry et al. 2002).

REFERENCES

Agawin, N.S.R., Agusti, S., Durate, C.M., 2002. Abundance of Antarctic picophytoplankton and their response to light and nutrient manipulation. Aquat Microb Ecol, 29, 161 - 172

Ahlgren N.A., Rocap G. 2006. Culture isolation and culture-independent clone libraries reveal new marine *Synechococcus* ecotypes with distinctive light and N physiologies. Appl Environ Microbiol, 72, 7193 - 7204

Alledredge, A.L., Passow, U., Logan, B., 1993. The abundance and significance of a class of large, transparent organic particles in the ocean. Deep-Sea Res. (1) ,40, 1131 – 1140

Andersen, P., Fenchel, T., 1985. Bacterivory by microheterotrophic flagellates in seawater samples. Limnol. Oceanogr. 30 (1) 198 - 202

Azam, F. , 1998. Microbial Control of Oceanic Carbon Flux: the Plot Thickness. Science. 280, 694 - 696.

Azam, F., Fenchel, T., Field, J.G., Gray, J.S., Mayer-Reil, L.A., Thingstad F.,1983. The ecological role of water column microbes in the sea. Mar. Ecol. Prog. Ser. 10, 257 - 263.

Azam, F., Fuhrman, J.A. 1984. Measurement of bacterioplankton growth in the sea and its regulation by environmental conditions. In "Heterotrophic activity in the sea", Hobbie J.E., Williams P.J. (eds), Plenum Publishing Corp, New York, p 179-196

Azam, F., Smith, D.C., Hollibaugh, JT., 1991. The role of the microbial loop in Antarctic pelagic ecosystems. Polar Res, 10, 239 - 243

Bec B., Husseini-Ratrema J., Collos Y., Souchu P., Vaquer A., 2005. Phytoplankton seasonal dynamics in a Mediterranean coastal lagoon: emphasis on the picoeukaryote community. J. Plank. Res. 27, 881-894.

Becquevort, S., Dumont, I., Tison, J.L., Lannuzel, D., Sauvée, M.L., Chou, L., Schoemann, V., 2009. Biogeochemistry and microbial community composition in sea ice and underlying seawater off East Antarctica during early spring. Polar Biol, 32, 879 - 895

Berninger U.G., Wickham S.A., 2005. Response of the microbial food web to manipulation of nutrients and grazers in the oligotrophic Gulf of Aqaba and northern Red Sea. Mar. Biol. 147, 1017-1032.

Boenigk, J., Arndt, H. 2002. Bacterivory by heterotrophic flagellates: community structure and feeding strategies. Antonie Van Leeuwenhoek 81: 465–480

Boyd P.W., 2002. Modelling regional responses by marine pelagic ecosystems to global climate change. Geophisical research letters. Volume 29, 53

Brandini FP, Rebello J., 1994. Wind field effect on hydrography and Chlorophyll dynamics in the coastal pelagial of Admiralty Bay, King George Island, Antarctica. Antarct Sci 6, 433–442

Budillon, G., Pacciaroni, M., Cozzi, S., Rivaro, P., Catalano, G., Ianni, C. & Cantoni, C., 2003. An Optimum Multiparameter Mixing Analysis Of The Shelf Waters In The Ross Sea. Antarctic Science, 15, 105 – 118

Burkill P.H., Edwards E.S., Sleight M.A., 1995. Microzooplankton and their role in controlling phytoplankton growth in the marginal ice zone of the Bellingshausen Sea. Deep Sea Research Part II: Topical Studies in Oceanography. 42, 1277-1290

Busseler O.K. and Boyd P.W., 2009. Shedding light on processes that control particle export and flux attenuation in the twilight zone of the open ocean. Limnology and oceanography. 54, 1210-1232

Boenigk, J., Arndt, H. 2002. Bacterivory by heterotrophic flagellates: community structure and feeding strategies. Antonie Van Leeuwenhoek 81: 465–480

Budillon, G., Castagno, P., Aliani, S., Spezie, G., Padman, L., 2011. Thermohaline variability and Antarctic bottom water formation at the Ross Sea shelf breack, Deep Sea Research Part I: Oceanographic Research Papers, 58, 1002 - 1018

Budillon, G., Gremes Cordero, S., Salusti, E., 2002. On the dense water spreading off the Ross Sea Shelf (antarctica), EGS XXVII General Assembly, 21 - 26

Calbet A., Landry M.R., 2004. Phytoplankton growth, microzooplankton grazing, and carbon cycling in marine systems. Limnol. Oceanogr. 49, 51-57.

Carmack, E.C., 1977. Water characteristics of the Southern Ocean south of the polar front. In: Angel, M. (Ed.), A Voyage of Discovery: George Deacon 70th Anniversary. Pergamon, Oxford, 15–41

Caron D.A., Dam H.G., Kremer P., Lessard E.J., Madin L.P., Malone T.C., Napp J.M., Peele E.R., Roman M.R., Youngbluth M.J., 1995. The contribution of micro organisms to particulate carbon and nitrogen in surface waters of the. Sargasso Sea near Bermuda. Deep-Sea Res. 42, 943-972

Caron, D.A., Peele, E.R., Lim, E.L., Dennet, M.R., 1999. Picoplankton and nanoplankton and their trophic coupling in surface waters of the Sargasso Sea south of Bermuda. Limnol. Oceanogr., 44, 259-272

Chisholm, S.W., Olson, R.J., Zettler, E.R., Goericke, R., Waterbury J.B., Welschmeyer N.A. 1988. A novel free-living prochlorophyte abundant in the oceanic euphotic zone. Nature, 334, 340 - 343

Christaki U., Vázquez-Domínguez E., Courties C., Lebaron P. 2005. Grazing impact of different heterotrophic nanoflagellates on eukaryotic *Ostreococcus tauri* and prokaryotic picoautotrophs *Prochlorococcus* and *Synechococcus*. Environ Microbiol 7: 1200–1210

Christaki, U., Giannakourou, A., Van Wambeke F. , Gregori, G., 2001. Nanoflagellate predation on auto- and heterotrophic picoplancton in the oligotrophic Mediterranean Sea. J. Plankton Res, 23, 1297 - 1310

Christaki, U., Jacquet, S., Dolan, J.R., Vaulot, D., Rassoulzadegan, F., 1999. Differential grazing and growth on *Prochlorococcus* and *Synechococcus* by two contrasting ciliates. Limnol Oceanogr 44, 52 – 61

Church, M.J., DeLong, E.F., Ducklow, H.W., Karner, M.B., Preston, C.M., Kark, D.M., 2003. Abundance and distribution of planktonic Archaea and bacteria in the waters west of the Antarctic Peninsula. Limnol Oceanogr, 48, 1893 - 1902

Collos Y., Husseini-Ratrema J., Bec B., Vaquer A., Hoai T.L., Rougier C., Pons V., Souchu P. (2005). Phaeopigment dynamics, zooplankton grazing rates and the autumnal ammonium peak in a Mediterranean lagoon. Hydrobiologia. 550: 83-93.

Daley R.J., Hobbie J.E., 1975. Directs counts of aquatic bacteria by a modified epifluorescent technique. Limnol. Oceanogr. 20, 875 - 882.

Davis, P.G., Sieburth, L.McN., 1984. Estuarine and oceanic microflagellate predation of actively growing bacteria: estimation by frequency of dividing-divided bacteria. Mar. Ecol. Prog. Ser., 19, 237- 246

Deacon, G.E.R., 1937. The hydrology of the Southern Ocean. Discovery Report. 15, 3 – 122.

Deacon, G.E.R., 1984. The Antarctic Circumpolar Ocean. Studies in Polar Research. Cambridge University, Cambridge, 180pp.

del Giorgio P.A, Gasol, J.M., Vaqué D., Mura P., Agusti S., Duarte C.M., 1996. Bacterioplankton community structure: Protists control net production and the proportion of active bacteria in a coastal marine community. Limnology and Oceanography. 41, 1169-1179

DeLong, E.F., Wu, K.Y., Prèzelin, B.B., jovine, R.V.M., 1994. High abundance of Archaea in Antarctic marine picoplankton. Nature, 371, 695 - 697

Dinniman, M.S., Klinck, J.M., Smith, W.O. ,Jr 2003. Cross-shelf exchange in a model of the Ross Sea circulation and biogeochemistry. Deep-Sea Res. II, 50, 3103 – 3120

Dolan J, Gallegos C.L., Moigis A., 2000. Dilution effects on microzooplankton in dilution grazing experiments. Mar Ecol Prog Ser 200, 127-139.

Doolittle, D.F., Li, W.K.W., Wood, A.M., 2008. Wintertime abundance of picoplankton in the Atlantic sector of the Southern Ocean. Nova Hedwig, 133, 147 - 160

Eppley, R.W., Horrigan, S.G., Fuhrman, J.A., Brooks, E.R., Price, C.C., Sellner, K., 1981. Origin of dissolved organic matter in the Southern California waters: experiments on the role of zooplankton. Mar. Ecol. Prog. Ser. 6: 149-159.

Evans G.T., Paranjape M.A., 1992. Precision of estimates of phytoplankton growth and microzooplankton grazing when functional response of grazers may be nonlinear. Mar. Ecol. Prog. Ser. 80, 285-290.

Fenchel T., 1982. Suspended marine bacteria as a food source. In: Fasham M.J.R. (Ed) Flows of energy and materials in marine ecosystems. Theory and practice. Pergamon Press., New York and London, 301 - 315

Fileman, E.S., Leakey, R.J.G., 2005. Microzooplankton dynamics during the development of the spring bloom in the north-east Atlantic. J. Mar. Biol. Assoc. U.K. 85, 741-753.

Fonda Umani S., 2000. From inorganic solution to hydrogel. Biol. Mar. Medit. 7 (1): 40 - 154.

Fonda Umani S., Malisana E., Focaracci F., Magagnino M., Corinaldesi C., Danovaro R., 2010. Disentangling the effect of viruses and nanoflagelattes on prokaryotes in bathypelagic waters of the Mediterranean Sea. Mar. Ecol. Prog. Ser. 418, 73-85

Fonda Umani, S., Tirelli, V., Beran, A., Guardiani, B., 2005. Relationships between microzooplankton and mesozooplankton: competition versus predation on natural assemblages of the Gulf of Trieste (northern Adriatic Sea). J. Plank. Res. 27, 973 - 986.

Foster, T.D., Carmack, E.C., 1976. Frontal zone mixing and Antarctic Bottom Water formation in the southern Weddell Sea, in: Deep Sea Research and Oceanographic Abstracts, vol. 23, 301 - 317, Elsevier

Frost B.W. , 1972. Effects of size and concentration of food particles on the feeding behaviour of the marine planktonic copepod *Calanus pacificus*. Limnol. Oceanogr. 17, 805-815.

Fuhrman, J.A., McManus, G., 1984. Do bacteria-sized marine eukaryotes consume significant bacterial production? Science, 224, 1257 - 1260

Fuhrman, J.A., Noble, R.T., 1995. Viruses and protists cause similar bacterial mortality in coastal seawater. Limnol. Oceanogr, 40, 1236 - 1242.

Fuhrman, J.A., Suttle, C.A., 1993. Viruses in marine planktonic system. Oceanography, 6, 51 - 63

Gallegos C.L., 1989. Microzooplankton grazing on phytoplankton in the Rhode River, Maryland: nonlinear feeding kinetics. Mar. Ecol. Prog. Ser. 57, 23-33.

Garces, E., Vila, M., Maso, M., Sampedro, N., Giacobbe, M.G., Penna, A., 2005. Taxon-specific analysis of growth and mortality rates of harmful dinoflagellates during bloom conditions. Mar. Ecol. Prog. Ser. 301, 67-79.

Gordon, A.L., Huber, B.A., 1990. Southern Ocean winter mixed layer. Journal of Geophysical Research 95, 11655 – 11672.

Gasol, J.M., 1994. A framework for the assessment of top-down vs bottom-up control of heterotrophic nanoflagellate abundance. Mar Ecol Prog Ser 113, 291 – 300

Hall J.A., Safi K., The impact of in situ Fe fertilisation on the microbial food web in the Southern Ocean. Deep Sea Research Part II: Topical Studies in Oceanography. 48, 2591-2613

Hammer O, Harper D.A.T. and Ryan P.D., 2001. PAST - PAlaeontological STatistics, ver. 1.89

Hewes, C.D., Sakshaug, E., Reid, F.M.H., Holm-Hansen, O., 1990. Microbial autotrophic and heterotrophic eucaryotes in Antarctic waters: relationship between biomass and Chlorophyll, adenosine triphosphate and particulate organic carbon. Mar Ecol Prog Ser, 63, 27 - 35

Hewes C.D., 2009. Cell size of Antarctic phytoplankton as a biogeochemical condition. Arctic science. 21, 457-470

Honio, S., Roman, M.R., 1978. Marine copepod fecal pellets: production, preservation and sedimentation. J. Mar. Res., 36, 45 - 57.

Ilango, V, Subramanian R, Vasudevan V., 2011. Cluster Analysis Research Design model, problems, issues, challenges, trends and tools. International Journal on Computer Science and Engineering 3.8, 3064-3070

Jacobs, S., Amos, A., Bruchhausen, P., 1970. Ross Sea oceanography and Antarctic bottom water formation, Deep - Sea Research, 17, 935 - 62

Jacobss, S., Fairbankrs, G., Horibe, Y., 1985. Origin and evolution of water masses near the Antarctic continental margin: evidence from H,180/H,'60 ratios in seawater. *Antarctic Research Series,* 43, 59 - 85.

Jochem F.J., Lavrentyev P.J., First M.R., 2005. Growth and grazing rates of bacteria groups with different apparent DNA content in the Gulf of Mexico. Mar. Biol. 145, 1213-1225.
.
Johnson, P.W., Sieburth, J.McN., 1979. Chroococcoid cyanobacteria in the sea: a ubiquitous and diverse phototrophic biomass. Limnol. Oceanogr. 24, 928 - 935

Kiørboe, T., 1996. Material flux in the water column. In: Eutrophication in Coastal Marine Ecosystem. Coastal and Estuarine Studies, 52, 67-94.

Kuuppo-Leinikki, P., 1990. Protozoan grazing on planktonic bacteria and its impact on bacterial population. Mar. Ecol. Prog. Ser. 63, 227 - 238

Landry M.R., Kirsctein J., Constantinou J., 1995. A refined dilution technique for measuring the community grazing impact of microzooplankton, with experimental tests in the central equatorial Pacific. Mar Ecol Prog Ser 120, 53-63

Landry, M.R., Hassett, R.P., 1982. Estimating the grazing impact of marine microzooplankton. Marine Biology 67, 283-288.

Landry M.R., Kirchman D.L., 2002. Microbial community structure and variability in the tropical Pacific. Deep Sea Research Part II: Topical Studies in Oceanography. 49, 2669-2693

Lannuzel, D., Schoemann, V., Dumont, I., Content, M., Jong, J., Tison, J.L., Delille, B., Becquevort, S., 2013. Effect of melting Antarctic sea ice on the fate of microbial communities studied in microcosms. Polar Biol, 36, 1483 - 1497

Legendre L., Rassoulzadegan F., 1995. Plankton and nutrient dynamics in marine waters. Ophelia, 41, 153 - 172

Legendre, L., 1996. The biological CO_2, pump in seasonally ice covered waters. Proc NIPR. Symp. Polar Biol., 9, 61-74.

Legendre, L., Le Fevre, J., 1992. From individual plankton cells to pelagic marine ecosystems and to global biogeochemical cycles. Demers S., (ed). Particle analysis in oceanog. Spinger-Vvrlag, Berlin. 261 - 300.

Leising, A.W., Horner, R., Pierson, J.J., Postel, J., Halsband-Lenk, C., 2005. The balance between microzooplankton grazing and phytoplankton growth in a highly productive. A method for continuous measurement of in vivo chlorophyll concentrations. Deep-Sea Res. 13, 223-227.

Locarnini, R.A., 1994. Water masses and circulation in the Ross Gyre and environs. Ph.D. Thesis, Texas A&M University, unpublished.

MacAyeal, D.R. , 1985. Evolution of tidally triggered meltwater plumes below ice shelves in Oceanology of the Antarctic Continental Shelf, Antarc. Res. Ser., vol. 43, 133-143

Mosby, H., 1934. The water of the Atlantic Antarctic Ocean. Scientific Results of the Norwegian Antarctic Expedition 1927–1928 (1), 131.

Murray, A.E., Preston, C.M., Massana, R., Taylor, L.T., Blakis, A, Wu, K.Y., DeLong, E.F., 1998. Seasonal and spatial variability of Bacterial and Archeal assemblages in the coastal waters near Anvers Island, Antarctica. Appl Environ Microbiol, 64, 2585 - 2595

Nagata T., Fukuda H., Fukuda R., Koike I. 2000. Bacterioplankton distribution and production in the deep Pacific waters: large-scale geographic variations and possible coupling with sinking particle fluxes. Limnol Oceanogr 45: 426-435

Orsi, A. H., Wiederwohl, C. L., 2003. A recount of Ross Sea waters. Deep-Sea Research II, 56, 778-795.

Orsi, A., Smethier Jr, W., Bullister, J, 2002. On the Total input of Antarctic Waters the deep ocean: A preliminary estimate from chlorofluorocarbon measurements, j. Geophys.

Res, 107, 3122.

Pomeroy L.R., 1974. The ocean's food web, a changing paradigm. BioSci. 24 (9): 499 -504.

Pomeroy, L.R., Williams, P.J.L., Azam, F., Hobbie, J.E., 2007. The microbial loop. Oceanography, 20, 28 – 33

Porter K.G., Feig Y.S., 1980. The use of DAPI for identifying and counting aquatic microflora. Limnol Oceanogr 25, 943-948

Price, B., Sowers, T., 2004. Temperature dependence of metabolic rates for microbial growth, maintenance and survival. PNAS, 101, 4631 - 4636

Rassoulzadegan F., 1993. Protozoan patterns in the Azam-Ammerman's bacteriaphytoplankton mutualism. In: Guerrero R., Perdo-Aliò C. (eds). Trends in Microb. Ecol., 435- 4 39.

Reinthaler T., van Aken H., Veth C., Williams P.J.Leb. 2006. Prokaryotic respiration and production in the meso and bathypelagic realm of the eastern and western North Atlantic basin. Limnol. Oceanogr. 51,1262–1273

Sanders, W.R., 1991. Mixotrophic Protists in Marine and Freshwater Ecosystems. j. protozool, Vol. 38, 76 - 81

Sherr,B.F., Sherr, E.B., Pedros-Alio, C., 1989. Simultaneous measurement of bacteria plankton production and protozoan bacterivory in estuarine water. Mar. Ecol. Prog. Ser. 54: 209 - 219.

Simon, M., Glockner, F.O., Amann, R., 1999. Different community structure and temperature optima of heterotrophic picoplankton in various regions of the Southern Ocean. Aqua Microb Ecol, 18, 275 - 284

Sleigh M.A. 2000. Trophic strategies. In "The Flagellates" Leadbeater B.S.C., Green J.C. (eds), Taylor & Francis, London, p 147–165

Smethie, W., Jacobs, S., 2005. Circulation and melting under the Ross Ice Shelf: estimates from evolving CFC, salinity and temperature fields in the Ross Sea, Deep Sea Research Part I: Oceanographic Research papers, 52, 959 - 978

Sohrin R., Imazawa M, Fukuda H., Suzuki Y., 2010. Full-depth profiles of prokaryotes, heterotrophic nanoflagellates, and ciliates along a transect from the equatorial to the subarctic central Pacific Ocean 57, 1537-1550

Strzepek, R.F., Maldonado, M.T., Higgins, J.L., Hall, J., Safi, K., Wilhelm, S.W., Boyd, P.W. , 2005. Spinning the ''Ferrous Wheel'': the importance of the microbial community in an iron budget during the Fe Cycle experiment. Glob. Biogeochem. Cy. 19 (Art. No. GB4S26).

Tanaka, T., 2009. Structure and function of the mesopelagic microbial loop in the NW Mediterranean Sea. Aquatic Microbial Ecology 57, 351-361.

Tonelli M., Wainer I., Curchitser E., 2012. A modelling study of the hydrographic structure of the Ross Sea. Ocean Science Discussion, 9

Troussellier M., Got P., Boup M., Corbin D., Giuliano L., Cappello S., Bouvy, M., 2005. Daily bacterioplankton dynamics in a sub-Saharan estuary (Senegal River, West Africa): a mesocosm study. Aquat. Microb. Ecol. 40, 13-24.

Volk T., Hoffert M.I., 1985. Ocean carbon pumps: analysis of relative strengths and efficiencies in ocean driven atmospheric CO2 change. In: ET. Sundquist, Broecker W.S. (eds), The Carbon Cycle and Atmospheric CO2; Natural Variations Archean to Present, Washington DC; American Geophysical Union, Geophysical Monograph., 32, 99 - 110.
.

Waterbury, J.B., Watson, S.W., Guillard, R.R.L., Brand, L., 1979. Widespread occurrence of a unicellular, marine, planktonic cyanobacterium. Nature, 277, 293 - 294.

Williams, P.J. Le B., 1990. The importance of losses during microbial growth: Commentary on the physiology, measurement and ecology of the release of dissolved organic material. Mar. Microb. Food Webs, 4, 175 - 206.

Worthington, L., 1981. The water masses of the World Ocean: Some results of a fine - scale census. Evolution of physical oceanography, 42 - 69

Wright, S.w., Ishikawa, a., Marchant, H.J., Davidson, A.T., Enden, R.L., Nash, G.v., 2009. Composition and significance of picophytoplankton in Antarctic waters. Polar Biol, 32, 797 - 808

Wüst, G., 1935. Schichtung und Zirkulation des Atlantischen Ozeans. Wissenschaftliche Ergebnisse der Deutschen Atlantischen Expedition des Forschungsschiffes 'Meteor' 1925-192. 6, 1 - 288.

Wynn-Williams, DD. 1996. Antarctic microbial diversity: the basis of polar ecosystem processes. Biodivers Conserv, 5, 1271 - 1293

Yacobi Y.Z., Zohary T., Kress N., Hecht A., Robarts R.D., Waiser M., Wood A.M., Li W.K.W. 1995. Chlorophyll distribution throughout the southeastern Mediterranean in relation to the physical structure of the water mass. J Mar Syst 6: 179-190

Yokokawa, T., Nagata, T. , 2005. Growth and grazing mortality rates of phylogenetic groups of in coastal marine environments. Appl. Environ. Microbiol. 71, 6799-6807.

Zdanowski, M.K., 1995. Characteristics of bacteria in selected Antarctic marine habitats. Polish Academy of Sciencesc, 5 - 100